Materials Today Bio 5 (2020) 100038

Contents lists available at ScienceDirect

Materials Today Bio

journal homepage: www.journals.elsevier.com/materials-today-bio

Materials and manufacturing perspectives in engineering heart valves: a review

F. Oveissi [a,d], S. Naficy [a,d,*], A. Lee [a,b,c], D.S. Winlaw [b,c], F. Dehghani [a,**]

[a] School of Chemical and Biomolecular Engineering, The University of Sydney, Sydney, New South Wales, 2006, Australia
[b] Discipline of Child and Adolescent Health, Sydney Medical School, Faculty of Health and Medicine, The University of Sydney, New South Wales, 2006, Australia
[c] Heart Centre for Children, The Children's Hospital at Westmead, New South Wales, 2145, Australia

ARTICLE INFO

Keywords:
Biofabrication
Biomaterials
Electrospinning
Valvular heart diseases
3D printing

ABSTRACT

Valvular heart diseases (VHD) are a major health burden, affecting millions of people worldwide. The treatments for such diseases rely on medicine, valve repair, and artificial heart valves including mechanical and bioprosthetic valves. Yet, there are countless reports on possible alternatives noting long-term stability and biocompatibility issues and highlighting the need for fabrication of more durable and effective replacements. This review discusses the current and potential materials that can be used for developing such valves along with existing and developing fabrication methods. With this perspective, we quantitatively compare mechanical properties of various materials that are currently used or proposed for heart valves along with their fabrication processes to identify challenges we face in creating new materials and manufacturing techniques to better mimick the performance of native heart valves.

1. Introduction

Valvular heart diseases (VHD) such as congenital, rheumatic, and degenerative heart diseases that lead to stenosis and regurgitation in heart valves demand continuous clinical attention. In economically developed societies, it is estimated that more than 30 million people live with VHD, where the incidence increases with age [1]. As an example, 1.5% of Americans and British people are diagnosed with VHD each year [1,2]. Almost 75% of VHD in adults involves dysfunction of the aortic and mitral valves [3]. In younger patients, 33% of congenital heart diseases are related to abnormalities of the aortic or pulmonary valves [1].

Heart valve repair is often preferred to heart valve replacement when sufficient tissue remains for reconstruction. However, in many VHD, the valve replacement is unavoidable. Although transcatheter treatments and minimally invasive operations have been clinically applied to patients with VHD, the majority of valve replacement surgeries resort to open heart approaches. Overall, more than 300,000 valve replacements per annum are performed for patients with severe valvular dysfunction [4,5], and there is still some hesitation in employing the transcatheter valve replacement in younger patients [6]. Also, transcatheter valves are needed to be significantly reduced in thickness due to their folded design, which would be a durability challenge. To this date, only mechanical and bioprosthetic valves have been used clinically while they often resulted in inconvenience and complications relating to anticoagulant intake, immune-driven calcification, and degradation [7]. Homografts obtained from human donors have also been used as alternatives for VHD, but are associated with drawbacks including the immunological response that eventually leads to structural valve deterioration, potential disease transmission, and limited supply. Somatic growth of infant and child recipients of heart valve replacement mandates several further surgeries

Abbreviations: α-SMA, alpha-smooth muscle actin; dECM, decellularized extracellular matrix; *E*, Young's modulus; ePTFE, expanded PTFE; Gal, galactose-α1,3-galactose; GelMa, gelatin methacrylate; HA, hyaluronic acid; HAVIC, human aortic valvular interstitial cells; MA-HA, methacrylated hyaluronic acid; NeuGc, N-glycolylneuraminic acid; P4HB, poly(4-hydroxybutyrate); PAAm, polyacrylamide; PCE, polycitrate-(ε-polypeptide); PCL, polycaprolactone; PE, polyethylene; PEG, polyethylene glycol; PEGDA, polyethylene glycol diacrylate; PGA, poly(glycolic acid); PHA, poly(hydroxyalkanoate); PLA, polylactide; PMMA, poly(methyl methacrylate); PPG, polypropylene glycol; PTFE, polytetrafluoroethylene; PU, polyurethane; SIBS, poly(styrene-b-isobutylene-b-styrene); SMC, smooth muscle cells; VHD, valvular heart disease; VIC, aortic valve leaflet interstitial cells; xSIBS, crosslinked version of SIBS.

* Corresponding author.
** Corresponding author.
E-mail addresses: sina.naficy@sydney.edu.au (S. Naficy), fariba.dehghani@sydney.edu.au (F. Dehghani).
[d] These authors equally contributed to this work (co-first authors).

https://doi.org/10.1016/j.mtbio.2019.100038
Received 5 September 2019; Received in revised form 26 November 2019; Accepted 27 November 2019
Available online 5 December 2019

to increase the size of the valve replacement [8]. Hence, there is an unmet demand for novel materials that resemble the biomechanics of native heart valve tissue. In this regard, it is desirable that novel materials have mechanical and hemodynamic properties that are similar to native heart valves.

Multiple studies have reported the implantation of artificial heart valves in preclinical animal models using natural (e.g. collagen, silk, and fibrin) and synthetic polymeric heart valves over the last decade [9–13]. The main objectives in these studies were to utilize a rapid manufacturing process, reduce the cost, control the degradation rate, and provide sufficient strength to endure *in vivo* conditions. The recent advances in materials fabrication such as additive manufacturing have provided opportunities for constructing complex 3D structures with predetermined properties that may be customized to the patients' needs [14].

While several review articles have been published in the area of cardiovascular tissue engineering [7,15,16], none has thoroughly discussed the materials and more specifically fabrication methods for artificial heart valves in a quantitative approach from an engineering perspective. Therefore, in this review, we first give an overview of human heart valves' geometries and their mechanical properties to appreciate better the complexity that exists in this organ. We then provide an insight into advances made in materials domain for designing artificial heart valves and the challenges that are encountered in translating such materials to viable products. Finally, various techniques that have been used for the fabrication of heart valves are compared, followed by a discussion on current challenges and future perspective.

2. Human heart valves

Every heart consists of four valves: tricuspid, mitral, pulmonary, and aortic valves (Fig. 1A). The aortic valve regulates the flow from the left ventricle to the aorta. The roles of tricuspid and mitral valves are to regulate the blood inflow from the left and right atrium into the ventricles, correspondingly. The pulmonary valve controls the outward flow from the right ventricle to the pulmonary artery. The mean circumference of normal adult tricuspid valves is ~11.95 ± 1.26 cm (M) and 10.40 ± 1.06 cm (F) [17]. The mitral valve has a saddle-shaped annulus with a local displacement of 4.8 ± 1.9 mm in normal adults and a mean circumference of ~10.15 ± 1.24 (M) and 9.11 ± 0.86 (F) [17,18]. The structures of pulmonary and aortic valves (Fig. 1B–D) are similar, and both are made from three semilunar leaflets within valve roots. Both pulmonary and aortic valves (Fig. 1B) have smaller circumferences than tricuspid and mitral valves. The circumference of pulmonary valves is ~7.77 ± 0.98 (M) and ~7.32 ± 0.86 (F), and that of the aortic valve is ~7.50 ± 1.04 (M) and ~6.80 ± 0.89 (F) [17]. The leaflets of the typical

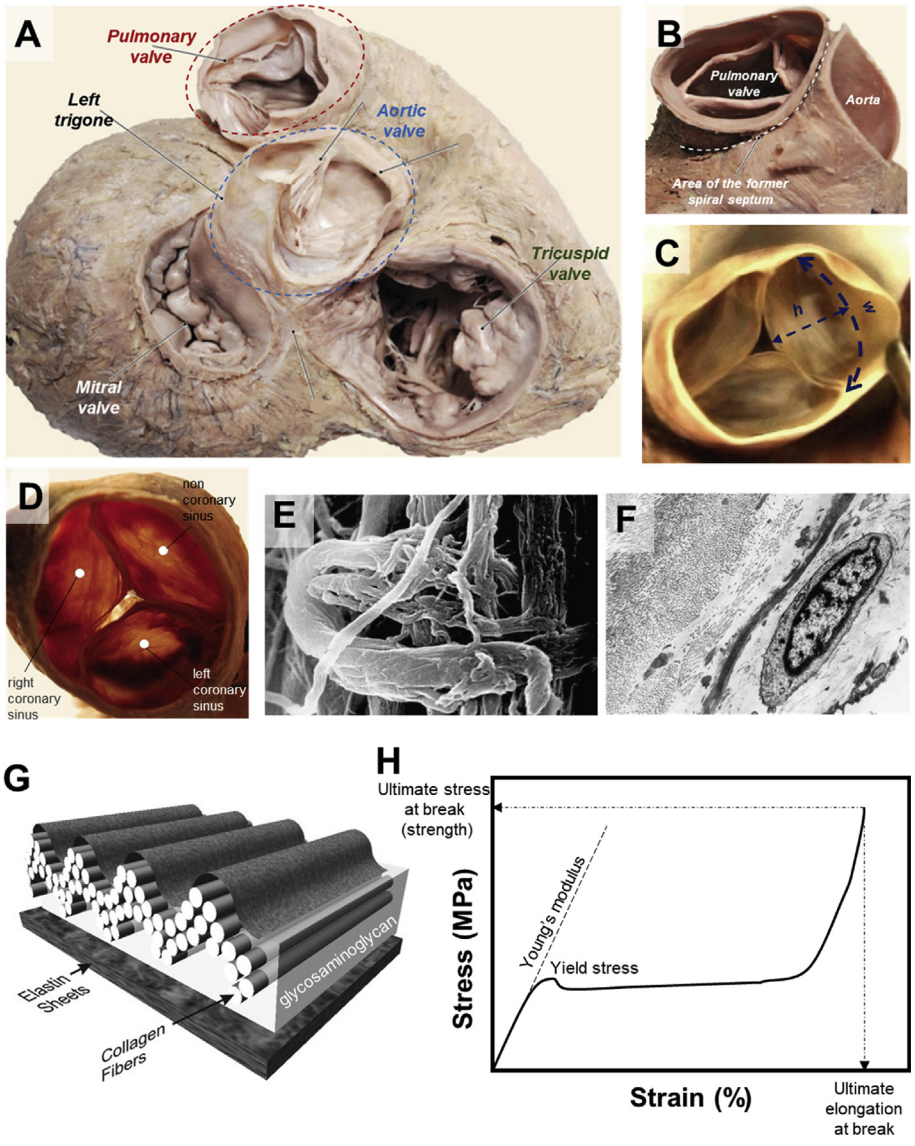

Fig. 1. Anatomy of human heart valves (A), the pulmonary valve in opened (B) and closed positions (C). The letters *h* and *w* in (C) refer to the height and the width, respectively. Superior view of aortic heart valve (D) with scanning electron micrograph image of the aortic valve cusp in its connection point with fibrous ring (E), demonstrating collagen fibers wrapped circularly on collagen in the inner part of the fibrous ring. Transmission electron micrograph of the pulmonary valve cusp (F), representing collagen fibers in transverse and longitudinal direction, elastic fibers in transverse section, and fibroblasts. Schematic diagram of the multilayered configuration of an aortic valve cusp, showing the location of the collagen fibers in the fibrosa, the elastin sheets in the ventricularis, and the glycosaminoglycan-rich matrix of the watery spongiosa (G). A model tensile stress–strain curve showing various mechanical parameters referred to throughout this review (H). Young's modulus indicates the stiffness, while ultimate stress and elongation at break highlight the maximum force and deformation endured by the material prior to complete failure. Figures in Panels A–D were modified [26], and Figures in Panels E–F [25] and Panel G [27] were adapted with permission from their publishers.

adult pulmonary valves, which composed of fibrosa, spongiosa, and ventricularis [19], have a width of ~22 ± 4 mm and a height of ~12 ± 2 mm (Fig. 1C) [20]. It should be noted that the given dimensions are merely an indicative average of the valves' geometry and vary in different individuals.

The main components of heart valves and their surrounding tissues (conduits) are collagen and elastin that create quite complex and highly anisotropic microstructures (Fig. 1E–G) [21–23]. The alignment and mechanical properties of these components affect the overall mechanical behavior of heart tissues such as Young's modulus, ultimate strain at the break, and ultimate stress at the break (Fig. 1H). The tensile mechanical properties of heart tissues are compared in Table 1. Given the highly complex architecture of heart valves, their mechanical performance is dominated by elastin at low-stress domain and tough collagen at high-stress region (Fig. 2). In general, both leaflet and wall tissues are stronger and stiffer in the circumferential direction than in the radial or axial directions [24]. For instance, for pulmonary leaflets, the modulus in the soft elastin phase is ~0.3 MPa in the radial direction and ~1 MPa in the circumferential direction, while the modulus in the stiff collagen phase is ~3.8 MPa in the radial direction and ~15.5 MPa in the circumferential direction. The ultimate failure stress for pulmonary leaflets is ~0.5 MPa in the radial direction and ~1.5 MPa in the circumferential direction. Similar trends exist for aortic valve leaflets, where stiffness and strength are considerably larger in the circumferential direction than in the radial direction (Table 1) [25]. The failure strain, a.k.a. the ultimate strain at the break, for valve leaflets is ~30% in radial direction and ~20% in circumferential direction. In contrast to valve leaflets, the walls are generally softer and more stretchable.

The hemodynamic properties of various sections of human hearts are listed in Table 2. The transvalvular pressure is the highest for the mitral position (~120 mmHg), followed by aortic (~80 mmHg), tricuspid (~25 mmHg), and pulmonary (~10 mmHg) [29]. Moreover, the cardiac valves undergo an extremely complex multi-axial stress regime comprised of bending and elongation with cyclic loading of approximately 3×10^7 cycle per year [30]. The peak shear stress applied *in vivo* to cardiac valves ranges between 0.3 and 150 Pa, while maximum stress [31,32] reaches 500 kPa with the radial and circumferential strains [31,33,34] around, respectively, 40% and 10%. Note that these values vary depending on the valve position.

3. Materials for artificial heart valves

The complex mechanical attributes of cardiac valves are a major challenge in the identification of suitable substitutes. In this section, various materials that have been used for the fabrication of heart valves at the before clinical stage are discussed with a special emphasis paid to their mechanical behavior.

Table 1
Biomechanical properties of aortic and pulmonary leaflets and walls in uniaxial tensile testing. The moduli of collagen and elastin phases are shown separately [25].

Cardiac valved conduit	Stiffness (MPa)		Strength (MPa)	Strain at break (%)
	Collagen	Elastin		
Aortic wall (axial)	1.72 ± 1.09	0.14 ± 0.10	0.72 ± 0.27	86.04 ± 15.26
Aortic wall (circumferential)	3.23 ± 0.74	0.19 ± 0.07	1.47 ± 0.68	89.14 ± 36.95
Pulmonary wall (axial)	2.14 ± 0.70	0.15 ± 0.18	0.83 ± 0.28	85.62 ± 27.88
Pulmonary wall (circumferential)	3.20 ± 3.95	0.10 ± 0.02	1.32 ± 1.28	93.29 ± 23.29
Aortic leaflet (radial)	1.30 ± 0.56	0.04 ± 0.04	0.19 ± 0.07	32.29 ± 8.18
Aortic leaflet (circumferential)	11.91 ± 7.18	0.36 ± 0.25	1.40 ± 0.56	21.29 ± 6.86
Pulmonary leaflet (radial)	3.81 ± 3.73	0.33 ± 0.75	0.53 ± 0.30	33.19 ± 13.78
Pulmonary leaflet (circumferential)	15.44 ± 9.72	1.07 ± 1.72	1.54 ± 0.84	17.12 ± 5.36

3.1. Mechanical heart valves

Mechanical heart valves are traditionally made of rigid materials with moduli significantly higher than those of human soft tissues. Early models of caged ball valves and non-tilting disc valves were generally made of methacrylate, nylon, stainless steel, stellite (cobalt-chromium-molybdenium-nickel alloys), titanium, ultrahigh-molecular-weight polyethylene, polytetrafluoroethylene, polyoxymethylene, Silastic (Dow Corning's proprietary silicon rubber), and silicone rubber [44]. Apart from the silicone rubber with modulus around 0.05 GPa, the rest of the components used in the manufacturing of caged ball valves and non-tilting disc valves had moduli exceeding 1 GPa. Heat treatment of silicon rubber after molding was introduced in 1968 to further cure the silicone balls and prevent lipid absorption, which resulted in deterioration and swelling of the ball in earlier models [45].

The current era of bileaflet mechanical valves are mostly made of stainless steel, titanium housing or pyrolytic carbon, leaflets of graphite coated with pyrolytic carbon, and an inner ring of 100% pyrolytic carbon [44]. All materials used in the fabrication of mechanical heart valves are selected for their favorable mechanical properties and biocompatibility. Specifically, pyrolytic carbon has been the biomaterial of choice for mechanical heart valves because of its resistance to surface thrombosis, superior strength (300–400 MPa) [46] and fatigue (10^5–10^9 cycles under stresses near fracture stress) [47,48]. Despite all desirable mechanical and biological properties, pyrolytic carbon is brittle with a fracture toughness of ~0.9–1.46 MPa $m^{1/2}$ [46,49–51], which is similar to that of brittle plastics such as polystyrene. Likewise, the ultimate strain at break of pyrolytic carbon is very low (<1%) compared to native cardiac leaflets (30–80%) [52].

The most common problem associated with mechanical valves is the risk of major bleeding from excessive therapeutic anticoagulation used to reduce the risk of thrombus formation [53]. The patient must receive a life-long anticoagulant treatment that increases the risk of bleeding with minor and major trauma. The use of oral anticoagulants during pregnancy in women with prosthetic valves is associated with fetal loss and congenital malformation [54].

3.2. Biologically derived heart valves

Aiming to reduce the thromboembolic complications of mechanical valves, xenografts and allografts were developed as alternatives. Allografts and xenografts, compared to mechanical heart valves, have fewer issues with the platelet adhesion and formation of thrombus [4].

In general, leaflet tissue and pericardium used as a valve substitute sourced from animals including pig, sheep, and cow are soft and more flexible. For instance, compared to the human aortic valve, the porcine aortic valve has lower radial and circumferential Young's moduli and larger elongations at break [19,52,55–59]. Decellularization has been advocated as a way of diminishing the intensity of the host immunological response; however, the physical and chemical processes involved lead to further deterioration of the mechanical properties of the bioprosthetic valves [25]. These bioprosthetic valves – typically derived from bovine pericardium, porcine pericardium, and porcine arterial valves – are then treated with a chemical crosslinking agent to increase their durability. The main consideration in choosing the crosslinking reagent is being low toxic while enhancing the mechanical properties, durability, and the stability of the xenograft. Examples of such crosslinkers are alginate azide, carbodiimide hydrochloride, glutaraldehyde, cyanimide1-ethyl-3(-3 dimethyl aminopropyl) adipoyl dichloride, hexamethylene diisocyanate, and glycerol.

Over the last decade, most studies in bioprosthetic heart valves have been focused on the role of galactose-α1,3-galactose (Gal), an antigen

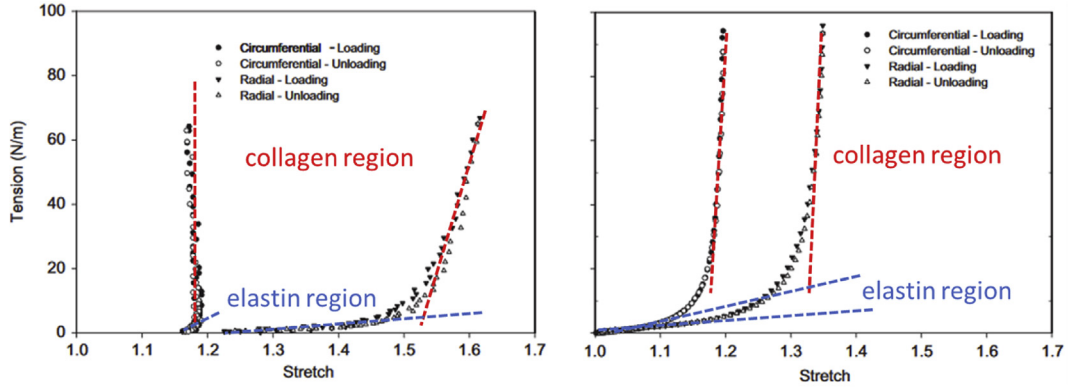

Fig. 2. Representative tension–stretch curves of aortic valve leaflets (left) and mitral valve anterior leaflets (right), highlighting the elastin-dominant and collagen-dominant regions [28]. Data presented here represent loading and unloading cycles where both curves overlap, indicating perfect recovery after deformation.

Table 2
Hemodynamic parameters for normal adult heart valves.

Heart valve	Blood flow rate (mL/s)	Peak blood velocity (m/s)	Transvalvular pressure (kPa)	Wall shear stress (Pa)
Aortic [35–37]	200	1.2	10.6	0.5–2
Mitral [38–40]	223	0.7	16	10
Pulmonary [41,42]	186	0.8–1.2	1.3	0.88
Tricuspid [43]	n.a.	0.49–0.51	3.3	n.a.

that contributes to xenograft rejection of tissues from pigs or cows by humans. McGregor et al. [60] and Lila et al. [61] demonstrated a link between Gal and calcification in heart valves. Also, they reported that the GT-KO (a genetically manipulated α-Gal deficient in pig pericardium), before labeled with human anti-Gal antibody, calcified less than pericardium without such treatment in a rat model – suggesting a new source of material for bioprosthetic heart valves [61].

It must be noted that the presence of "non-Gal" antigens such as N-glycolylneuraminic acid (NeuGc) is equally important as removing the Gal antigens [62,63]. Recently, genetically modified pigs that express neither Gal nor NeuGc have been produced and have been investigated as a potential xenograft source for bioprosthetic heart valves [64,65]. Cooper and coworkers [66] reviewed several genetically modified pig studies and compared the feasibility of potential genetic engineering approaches to reduce the human pathobiological responses to transplanted pig tissues. They suggested that xenoantigen deletion would be the most feasible genetic modification, though more studies were recommended [66].

3.3. Polymeric heart valves

Polymeric cardiac valves were originally introduced in 1952 in the form of polyethylene (PE) or poly(methyl methacrylate) (PMMA) balls enclosed in a PMMA tube. Both PMMA (Young's modulus ~3 GPa) and PE (~1 GPa) are rigid polymers [67] with moduli 10^2–10^5 times higher than those of native cardiac valve elements (~2–15 kPa) [24,68]. Later, the trileaflet polymeric valves were evolved as cardiac valve substitutes that better resembled the native geometries, hence could be hemodynamically more effective. The critical parameters in selecting suitable materials for polymeric heart valves include robust mechanical properties to retain structural integrity over repeated cyclic loading–unloading (e.g. negligible creep, high toughness, self-recovery), life-long anti-coagulation, and modulus close to native valve and conduit tissues. Compared to bioprosthetic valves, polymeric valves may be custom-designed to fit the requirements of specific patients and be less prone to calcification and failure. The most common materials include polyurethane, polytetrafluoroethylene, poly(styrene-*b*-isobutylene-*b*-styrene), biodegradable elastomers, and different types of hydrogels; the advantages and disadvantages of using each of these materials along with their mechanical behavior are fully discussed in the following sections.

3.3.1. Polyurethanes

Polyurethanes (PU) are obtained from the reaction between isocyanates (–N═C═O) and compounds with active hydrogen atoms (e.g. alcohols or amines). Urethane bonds result from the reaction of isocyanate and alcohol groups, while urea bonds are formed from the reaction of isocyanate with amine groups. Isocyanates used in the synthesis of polyurethanes can be either aliphatic or aromatic. Compared to aliphatic isocyanates, aromatic isocyanates result in mechanically superior polyurethanes but, in turn, have increased toxicity. Polyols used in the production of polyurethanes can have a backbone of polyesters (PLA, PGA, and PCL), polyols (PEG or PPG), polycarbonates, polydimethylsiloxane, or polybutadiene. The common members of polyurethane family that have been used in the fabrication of heart valves include polyester urethanes, polyether urethanes, polycarbonate urethanes, and polyether urethane urea (Scheme 1) [69–71].

In general, polyester urethanes have good viscoelastic properties but are prone to hydrolysis because of the ester bonds on their backbone. Polyether urethanes, on the other hand, have good resistance to hydrolysis but have low oxidation resistance. Polycarbonate urethanes address the hydrolysis and oxidation issues of polyester urethanes and polyether urethanes but remain susceptible to calcification. The first generation of PUs used in biomedical applications was ester-based, which presented low life cycle because of rapid hydrolysis [72]. One of the earliest examples of flexible polymeric cardiac valves was demonstrated by Braunwald and colleagues in 1960 [73], where a trileaflet polyurethane valve was used to replace a mitral valve. Later, Biomer® was used to fabricate ~80 μm thick leaflets for the pulmonary position [74]. Biomer® was a polyether urethane urea, composed of polytetramethylene ether glycol soft segments, aromatic hard segments, and amine chain extenders [75,76], which was marketed by Johnson & Johnson's Ethicon as a biomedical grade polyurethane. DuPont Biomer® was withdrawn from the market in 1991 mainly because of the common cracking failure, which revealed to be common in polyether urethanes. Mackay et al. [77] used solution casting and injection molding to prepare trileaflet PU heart valves made of Lubrizol Estane® 58201 (BF Goodrich), which could withstand 4×10^8 to 5×10^8 cycles of accelerated fatigue test (12 Hz, 100–120 mmHg pressure, with PU valves completely opening and closing in each cycle). Estane® 58201 has hard segments of 4,4′-diphenylmethane diisocyanate, soft segments of poly(tetramethylene glycol) and butanediol chain extenders [78]. Lubrizol Estane® 58201 also has suitable mechanical properties including high elongation at break (680%),

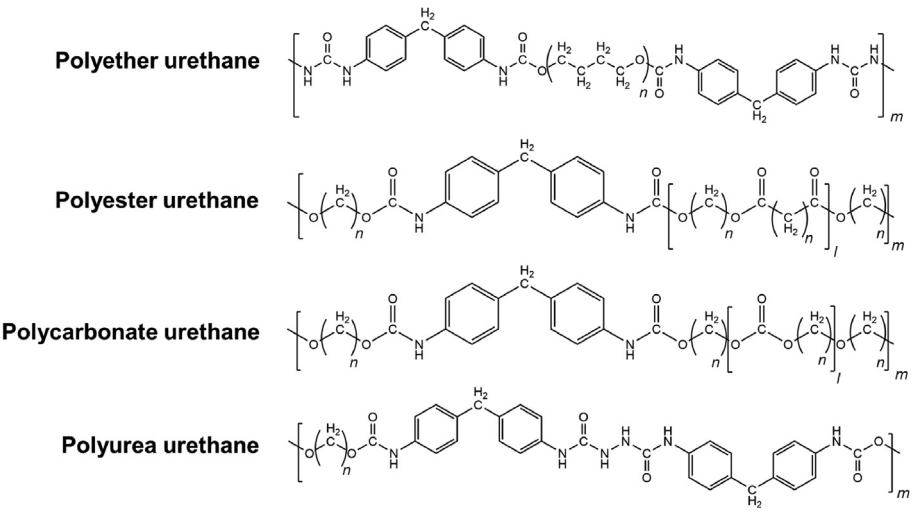

Scheme 1. Chemical structures of common polyurethanes used in the fabrication of hearts valves.

high toughness (44 kJ m^{-2}), and moderate strength (tensile strength ~39 MPa). With a modulus of ~3.8 MPa (at 50% strain), PU leaflets with ~100 μm thickness could provide superior resistance against the backflow in a pulse duplicator when compared to mechanical or bioprosthetic valves [77].

In another study, PU heart valves made of Angioflex® (a proprietary PU developed by ABIOMED Inc.) exhibited lower levels of calcification compared to certain tissue valves [79], although calcification of the polyurethane leaflets has been reported by others [80]. In an attempt to reduce calcification rate, anticalcification agents such as bisphosphonate [81] (2-hydroxyethane bisphosphonic acid) and heparin were covalently bound to the PU backbone [79]. Microscopy and X-ray results, however, indicated that calcification increased in the presence of bisphosphonic (Fig. 3A) during *in vitro* accelerated life testing [79].

Polycarbonate urethanes such as Bionate® exhibit considerably lower rates of biodegradation compared to other classes of PUs [83,84], enabling fabrication of thinner leaflets. Polycarbonate urethanes of various stiffness (from Adiam Life Science, Erkelenz, Germany) were used to fabricate bi- and tri-leaflet mitral [85] and aortic [82] heart valves. A combination of dip-coating of dropping techniques was used to generate a multilayered configuration made of polycarbonate urethanes with varying stiffness. Leaflets with a thickness of 100 μm–300 μm remained durable *in vivo* although exhibited mild calcifications (Fig. 3B).

Compared to polyether urethanes, polyether urethane urea is less likely to fail by cyclic mechanical fatigue [69]. Overall, PU-based valves exhibited high durability ranging between 10^8 and 8×10^8 cycles, depending on the type of PUs and their fabrication process [86]. To reinforce the leaflets, metallic or polymeric meshes such as polytetrafluoroethylene can be incorporated into the PU matrix (e.g. Roe–Moore and McGoon prosthesis) [87]. Such reinforced structures were expected to extend the life span and be more robust under mechanical loads. Reinforced nanocomposite PUs based on polyhedral oligomeric silsesquioxanes have also shown favorable biocompatibility and mechanical durability. The nanocomposites exhibited ~60% enhancement in ultimate strength (~50 MPa), higher stiffness (~26 MPa), improved elongation at break (~700%), enhanced tear resistance, and antithrombogenicity [88,89].

3.3.2. PTFE

Polytetrafluoroethylene, also known as Teflon® by DuPont's registered trademark, is a highly stable fluorinated polymer with low surface energy (Scheme 2). PTFE is a crystalline polymer (~40–70%), with nonlinear mechanical properties that exhibit temperature and rate-dependent modulus and yield stress. At room temperatures, PTFE has Young's modulus of ~1 GPa, the yield stress of ~10 MPa, ultimate stress of ~160 MPa, and strain at break of ~150% [90,91]. The low surface energy of PTFE results in a very low friction coefficient and non-adhesiveness, and its inertness makes it a suitable candidate for many medical applications, including in cardiovascular engineering.

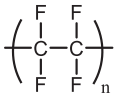

Scheme 2. Chemical structure of polytetrafluoroethylene (PTFE).

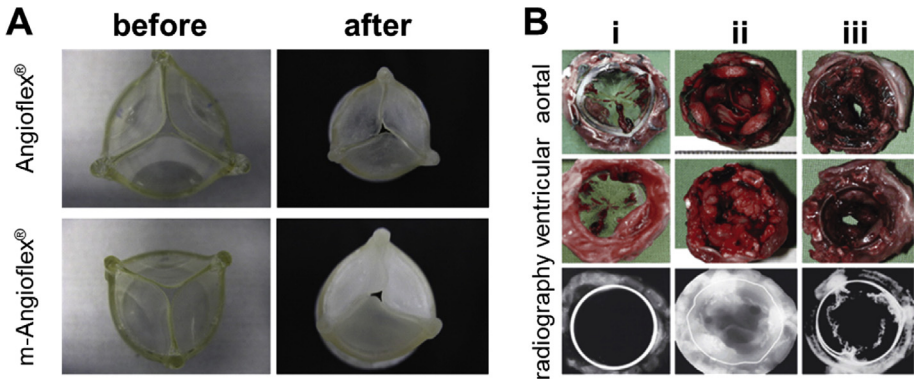

Fig. 3. Angioflex® and bisphosphonate-modified Angioflex® (polyether-based polyurethane) valves before and after calcification (A) [79]. Further examination revealed that the nature of calcification differs between the two materials. (B) Polycarbonate urethane heart valves after 20 weeks of implantation (i) compared with Mosaic® after 10 days (ii) and Perimount® after 30 days (iii) [82]. No visible calcification could be detected for polycarbonate urethane in radiography compared to Moasic® and Perimount® samples.

One of the very first examples of PTFE-based prostheses used to replace cardiac valves in patients was reported by Braunwald and Morrow in 1965 for aortic valves. However, valves failed due to calcification, tearing, and stiffening [92]. In 1969, the expanded PTFE (ePTFE) was introduced to the market by Bob Gore and since then has been widely recognized as Gore-Tex® products. Similarly, ePTFE trileaflet valves implanted in dogs [93] and sheep [94] showed calcification and stiffening, with both host cells and calcium infiltrated the micropores of the ePTFE. The ePTFE bicuspid pulmonary valves implanted in children and adults with congenital heart disease showed overall successful outcomes, especially in terms of valve regurgitation [95–97]. Nevertheless, despite good hemodynamic properties, both PTFE and ePTFE exhibit low resistance to thromboembolism and calcification (Fig. 4) [97].

3.3.3. SIBS

Poly(styrene-*b*-isobutylene-*b*-styrene) is a thermoplastic block copolymer (Scheme 3) now produced by Innovia. Initially, SIBS was introduced to address the *in vivo* degradation of polyurethanes since it does not have any reactive pendant groups [98]. SIBS reinforced with polyethylene terephthalate (Dacron®) was used for the fabrication of trileaflets for the aortic position of sheep [99]. However, the animal study results were not satisfactory with most valves failed because of calcification, creep, and material failure. This material was highly inert with no evidence of biodegradation. To address the occurring issue of creep in uncrosslinked SIBS [100], Innova introduced the crosslinked version of SIBS, which is referred to as xSIBS. Compared to SIBS, xSIBS has no creep, exhibits non-linear hyperelasticity, a wide range of elastic modulus (1.5–3 MPa), high strength (~5 MPa), and high elongation at break (100%<). *In vitro* hemodynamical evaluation of trileaflet valves made from xSIBS revealed no significant difference between the platelet activation of xSIBS valves and native tissue [101].

3.3.4. Biodegradable elastomers

Biodegradable elastomers promise to combine the highly sought-after mechanical properties needed for heart valve fabrication with controlled biodegradation to allow for growth of native tissue. One example of biocompatible and biodegradable elastomer is polycitrate-(ε-polypeptide) (PCE) with antibacterial activity and photoluminescent capacity. Because of its biocompatible backbone (polycitrate and polypeptide), PCE was found to be highly cyto- and hemo-compatible *in vitro* and showed low inflammatory response *in vivo* [102].

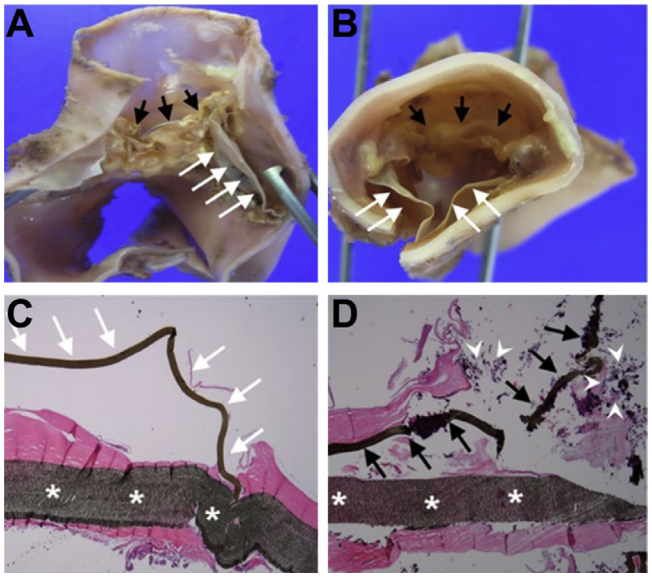

Fig. 4. Histopathological examination of ePTFE pulmonary valved conduits after explantation from young patients (median age of 25.3 months). Macroscopic (A, B) and microscopic (C, D) findings: white arrows indicate normal ePTFE valve cusp while black arrows indicate calcified ePTFE valve cusps. The white asterisks in (C, D) show the conduit wall and the white arrow heads point to infiltrated calcium [97].

Poly(hydroxyalkanoate) (PHA), a class of hydroxyl-alkanoic acid polyesters, can also be considered as biodegradable elastomers depending on their chemical structure (Scheme 4). Depending on the alkyl units in their backbones, PHAs range from highly crystallized rigid polymers to flexible elastomers.

PHAs are mainly derived through bacterial fermentation and their molecular structure can be determined by the fermentation feed. Pure PHAs intrinsically have excellent biocompatibility, and for most members of this family, the by-product of their degradation is a natural human metabolite [103,104]. Because of the ester group in their backbones, however, all PHAs are prone to hydrolysis. Hence, polyesters are mostly used to fabricate absorbable scaffolds for heart valves to incorporate fibroblasts and endothelial cells [105,106]. Among different members of PHA family, poly(4-hydroxybutyrate) (P4HB) is a thermoplastic elastomer with elongation at break of 10^3%, tensile modulus of 70 MPa, and tensile strength of 50 MPa [107]. Because of its desirable mechanical properties compared to innate heart valve tissues, P4HB has been attempted for the fabrication of functional living heart valves. In an example, non-woven poly(glycolic acid) (PGA) mesh was coated with P4HB to prepare an absorbable trileaflet heart valve scaffold for myofibroblasts and endothelial cells [108]. PGA itself is a biodegradable aliphatic polyester with a glass transition temperature within the range of 35–40 °C and crystallinity between 0 and ~50% [109]. Because of its favorable mechanical properties and bioabsorbability, PGA has been widely used in biomedical applications (e.g. first absorbable suture). Compared to PGA, P4HB has a longer absorption time (5–6 months vs 6–8 weeks) [110,111]; hence, the P4HB-coated PGA scaffolds could withstand the localized pressures and delay rupture [108]. The constructs resembled microstructure of normal heart valves and remained functional *in vivo* for up to 5 months in the descending aorta of juvenile sheep [112]. Yet, PHA family lacks internal crosslinking and still suffers from short life cycles.

3.3.5. Hydrogels

Hydrogels are three-dimensional networks made from highly hydrophilic polymers enabling them to contain a noticeable amount of water. Depending on their network topology and chemical structure of polymer backbones, the mechanical properties of hydrogels range from brittle with low fracture energies (10–100 J m^{-2}) to extremely tough with fracture energies similar to those of rubbers (~100–10000 J m^{-2}) [113]. The stiffness of hydrogels is largely controlled by their crosslinking ratio (physically or chemically) varying from ~1 kPa to 1–10 MPa. This range of moduli overlaps with the modulus of various human soft tissues [114]. Moreover, the swollen network of hydrogels allows for rapid diffusion of nutrients and oxygen, making them suitable candidates for tissue engineering and medical applications. Despite their high potentials, conventional hydrogels (e.g. ionically crosslinked alginate or chemically crosslinked polyacrylamide) suffer from brittleness [115]. Thus, many hydrogel systems that have been used in cardiac applications merely act as biocompatible scaffolds for cell support [116–118].

Hydrogels can be processed via a versatile range of fabrication methods such as electrospinning, molding, and bioprinting [119–121]. For instance, gelatin hydrogel composites reinforced with P4HB elastomeric fibers were developed through a two-step manufacturing process in which P4HB and gelatin fibers were electrospun on rotating collecting mandrels with desired valve geometry via a rotating fiber extrusion needle [122]. The mechanical properties of the composites could be tuned via spinning angle and electrospun fiber composition, with modulus ranging from 35 MPa for aligned P4HB fibers to ~200 kPa for radially oriented P4HB:gelatin 40:60 fibers. The fabricated fibers were attached to stents and deployed minimally invasively to the pulmonary position of an ovine model via transapical access. The deployed valve remained functional in its position for 15 h [122].

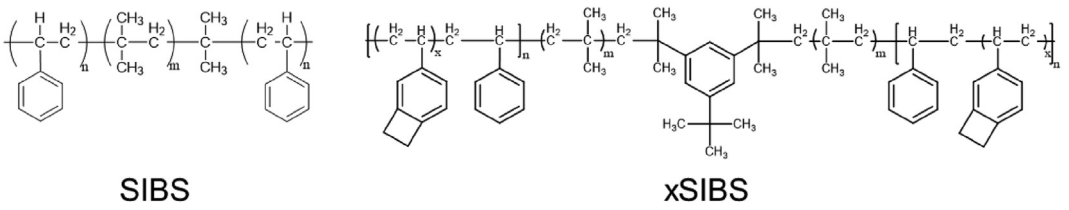

Scheme 3. Chemical structures of SIBS and xSIBS.

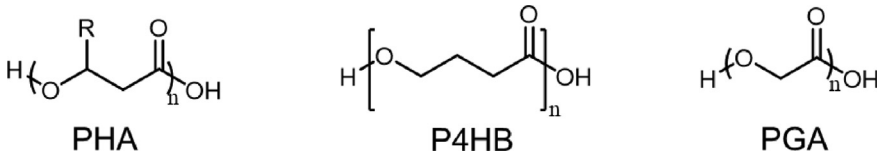

Scheme 4. Chemical structure of biodegradable ester elastomers: poly(hydroxyalkanoate) family (PHA), poly(4-hydroxybutyrate) (P4HB), and poly(glucolic acid) (PGA).

To fabricate heart valves as a whole through a seamless method, elastin-like recombinant-fibrin hydrogels were synthesized in a modular mold with the desired geometry of heart valves. This approach would also allow for the creation of multilayered constructs [123], or can be combined with electrospinning to achieve reinforced valved conduits [124]. Cell-laden alginate-gelatin hydrogels were 3D printed into hybrid valved conduits using a multimaterial 3D printer (Fab@Home™) [125]. Freshly prepared hydrogels with no cells had a modulus of ~1.4 MPa, but when incubated, their modulus declined rapidly over time, reaching ~1 MPa after 7 days. Similar trends were observed for ultimate strength and strain at break. The deterioration of mechanical properties of physical hydrogels (e.g. alginate) over time is a limiting obstacle in utilizing them for heart valve applications without any further reinforcement.

Various strategies have been developed to improve the toughness of hydrogels, such as nanocomposite hydrogels [126] and double-network hydrogels [127]. These strategies can be adapted to enhance the toughness of biocompatible but brittle hydrogels such as collagen. For instance, tough poly(ethylene glycol)-collagen double network hydrogels with considerably higher toughness compared to their constituting networks were prepared by polymerizing poly(ethylene glycol) diacrylate inside collagen hydrogels [128]. Depending on the ratio of collagen and poly(ethylene glycol) networks, ultimate strength could approach 800 kPa for highly swollen hydrogels with more than 96% water content.

Among various tough hydrogel systems, those capable of retaining their mechanical stability over dynamic loading are most suitable for cardiac valve applications. Dual crosslinked networks made of a physically crosslinked network with renewable crosslinking and a covalently crosslinked network with permanent crosslinking are one of such promising categories of tough hydrogels [129]. Under dynamic loading, the physical crosslinking (e.g. ionic, hydrogen bonding, hydrophobic) [130–136] can dissociate, dissipating a large amount of energy. On the other hand, the elastic network of covalently crosslinked polymers will act as the scaffold to bring back the material to its original structure after the load is removed. The physical crosslinks will be then reform, leading to the recovery of the system. One early example is highly stretchable hybrid hydrogels made of an ionically crosslinked alginate integrated with a covalently crosslinked polyacrylamide (PAAm) network [137,138]. The alginate-PAAm hybrid hydrogels exhibited very high fracture energies (~8000 J m^{-2}) at their optimum concentration and could recover their network structure after extreme deformation albeit at elevated temperatures (60–80 °C) and over long periods of time (~1 day). The modulus could be tuned by altering the ratio of alginate to PAAm, ranging from 20 kPa to 100 kPa. Protein-based tough hydrogels could also be achieved by dual crosslinking of unstructured elastin-like peptides using covalent and ionic crosslinking [139]. The physical and mechanical properties of protein-based dual crosslinked hydrogels could be tuned by the ratio of two networks and the level of ionic and covalent crosslinking. At high levels of ionic crosslinking, modulus could reach 80–120 kPa, and fracture energy picked at 1200 J m^{-2}. Hybrid hydrogels based on covalently crosslinked poly(ethylene glycol)-fibrinogen and supramolecular guest–host hyaluronic acid network may also exhibit recoverable mechanical performance [140], because of the renewable guest–host crosslinking. Another example is a semi-interpenetrating tough hydrogel system, which comprised of a physically and a chemically crosslinked network with fracture energy up to 1200 J m^{-2} and Young's modulus ranging from 1 to more than 10^3 kPa [114,141].

To summarize this section, Table 3 lists various materials with fabrication methods for heart valves in the ovine model. It should be noted that while the porcine model presents similarities to human in endothelialization and immune responses, the ovine model has been widely chosen for assessing the heart valves. The main reason for favoring ovine model is the high level of calcium and phosphorus in the serum, which would increase the calcification and may represent the worst scenario for heart valves. In general, ovine models are more aggressive animal models for testing the durability of engineered valves.

4. Manufacturing heart valves

Despite all advances in materials science and manufacturing, so far only mechanical and bioprosthetic heart valves have been used clinically. On-X® aortic heart valves by CryoLife are a recent example of mechanical heart valves with a 90° of leaflet opening to promote laminar hemodynamics. The leaflets are also made of pure pyrolytic carbon to achieve a smoother surface. In another class, low-profile Carpentier-Edwards® xenograft heart valves have exhibited promising performances. These xenografts are made of bovine pericardium leaflets secured by cobalt-chromium alloy stents, which are covered with polyester cloth and silicone rubber sewing rings. The leaflets are designed to improve durability and hemodynamics while the flexible cobalt-chromium alloy casing is intended for energy absorption and reduction of stress in leaflets.

For the next generation of artificial heart valves based on polymeric materials, molding, electrospinning, and additive manufacturing are the main fabrication methods that can be used for manufacturing of customized heart valves. In this section, the practical application of each of these methods in the fabrication of heart valves is discussed along with various materials that are compatible with each fabrication technique.

4.1. Molding

Molding has been extensively used for the fabrication of complex polymeric components. In this method, the polymeric solution or melt is

Table 3
Several preclinical studies of various fabricated materials for heart valves in the ovine model.

Material	Fabrication	Procedure	Sample size (N)	Significant outcome
Non-woven PGA meshes coated with 1.75% P4HB seeded with autologous bone marrow mononuclear cells [10]	Casting	Aortic valve replacement	After 12 h (N = 1), after 4 weeks (N = 5)	Early cellular infiltration and in-growth into the material; formation of layered endothelialized tissues; adequate mobility of leaflets.
Decellularized matrix, made from fibrin gel [11]	Casting	Pulmonary valve replacement	N = 8	The valve functioned well up to 8 weeks (4 weeks beyond the half-life of suture strength).
Non-woven PGA meshes coated with 1.75% P4HB seeded with ovine vascular-derived cells [12]	Casting	Pulmonary valve replacement	One-day follow-up (N = 2), after 8 weeks (N = 2), after 16 weeks (N = 4), and after 24 weeks (N = 4)	Mild central regurgitation was observed after week 8, followed by moderate progressing by week 24. Significant host cell repopulation was reported.
Polyglactin-PGA seeded with fibroblasts and SMCs followed by endothelial cells [105]	Casting	Right posterior leaflet of the pulmonary valve replacement	N = 4	No evidence of stenosis and trivial pulmonary regurgitation was observed. Development of extracellular matrix was confirmed by collagen analysis.
PGA and PLA seeded with mesenchymal stem cells [13]	Casting	Pulmonary valve replacement	N = 1	The mean collagen density in the circumferential direction was greater than that of the native pulmonary valve.
PHO seeded with vascular endothelial cells [142]	Casting	Pulmonary valve replacement	N = 4 (explanted after 1, 5, 13, and 17 weeks)	An increase in the inner diameter, the length, and the area of conduits was observed.
PGA and PHA as conduit and PHA as leaflet seeded with autologous endothelial cells [143]	Casting	Pulmonary valve and pulmonary artery replacement	N = 8 (explanted after 1, 2, 4, 6, 8, 12, 16, and 24 weeks)	No thrombus formation up to 24 weeks was observed.
2-Ureido-4[1H]-pyrimidinone-polyester urethane [144]	Electrospinning	Pulmonary valve replacement	3 months follow-up (N = 9) and 12 months follow-up (N = 7).	Partial material resorption and leaflet collagen replacement were observed.
Polycarbonate (modified with bis-urea) on a polyether ether ketone supporting stent; seeded with fibrin gel [145]	Electrospinning	Pulmonary valve replacement	2 months follow-up (N = 1), 6 months follow-up (N = 5), and 12 months follow-up (N = 4)	The implant was gradually substituted by layers of collagen and elastic matrix.
P4HB and gelatin [122]	Electrospinning	Pulmonary valve replacement	Acute (N = 4)	Hemodynamic performance was satisfactory. The valve was shown to be functional for 15 h in the ovine model.
Poly(L-lactide-*co*-D,L-lactide) nanofibers seeded with adult stem cells driven from bone marrow [146]	Electrospinning	Pulmonary valve replacement	8 weeks (N = 6)	Thickened leaflets, the formation of layered neotissues with endothelialized surfaces were reported.

introduced into a mold with the desired geometry and when the polymer is solidified after a certain time, then the construct is released from the mold. Multimaterial structures can be developed by utilizing a multistep approach through which different polymers are introduced to the mold at various times. For instance, multicomponent heart valves made of fibrin and elastin-like recombinant gels were produced as a proof-of-concept using multistaged injection molding (Fig. 5) [147]. Using such method, different types of cells and materials were employed to reconstruct the heterogeneity of the native heart valves. Additionally, the fabrication process of molding is generally very mild leading to high viability for embedded cells. Nevertheless, there are practical limitations in molding methods for constructing a highly heterogeneous structure made of multiple layers with different properties and cell types that could resemble the native heart valves (see Fig. 1G) [24]. The multistep molding process may require opening and closing of the mold several times leading to potential complications and discrepancy in manufacturing, which is not desirable. Moreover, while multicomponent constructs can be made via molding, each material phase will exhibit isotropic properties. In contrast, the native heart valves are multicomponent and anisotropic in each phase.

4.2. Electrospinning

Electrospinning is another highly versatile and efficient fabrication technique, which can be easily scaled up. Prior to the prevalence of electrospinning, other fabrication techniques such as drawing [148,149]

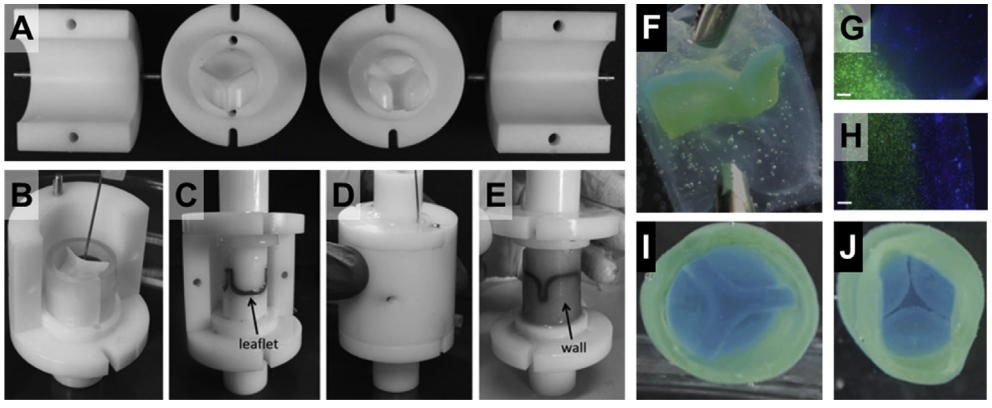

Fig. 5. Multistep injection molding for construction of a multimaterial heart valve. Mold parts are fabricated based on the desired valve geometry (A), followed by staged injection of different polymers as required (e.g. fibrin and elastin-like gels) (B–E). After solidification (e.g. gelation), the construct is released from the mold (F). Various cell types can be incorporated into the precursors before injection. The junctions between the leaflets and the wall and the structure of a two-layer leaflet are shown in (G) and (H), respectively, with two different cell populations, where nuclei of cells were stained blue (Hoechst 33258) and their cytoplasm was stained green (calcein AM). The vascular and ventricular sides of the valve are presented in (I) and (J). Scale bars are 200 μm. All figures were modified and reprinted with permission from the publisher [147].

had been used to obtain submicrometer fibers. However, electrospinning made it possible to continuously produce submicron to nanometer fibers from a wide range of polymeric materials [150]. Numerous natural biopolymers and synthetic polymers have been used in electrospinning by optimizing the solvent system and fabrication parameters. Examples of biopolymers that have been processed by electrospinning include collagen [151], chitosan [152,153], gelatin [154], fibrinogen [155], chitin [156], hyaluronic acid [157], and silk [158]. Yet, very few of such polymers have been used for the fabrication of heart valves.

Various polymeric materials have been processed via electrospinning for cardiac tissue engineering [159,160]. The microfibril structure of electrospun scaffolds is believed to provide a suitable environment to support myocardial tissue as it resembles the hierarchical structure of the myocardial tissue with aligned fibrous cells embedded in 3D honeycomb-like matrix of undulated perimysial collagen fibers and different ECM proteins [161,162]. The alignment of electrospun microfibers can be controlled to create mechanical anisotropy. Such microscale directionality in stiffness is particularly important for cardiac cells as they are responsive to mechanical cues from the environment [163]. In one study, electrospun scaffolds with bending stiffness ranging from ~2000 kPa to ~5000 kPa were fabricated from biodegradable polyester urethane by controlling the fiber insertion density during fabrication [164]. Various strategies can be applied for tuning the mechanical and biological properties of the scaffolds. For instance, Sant et al. used a standard setup to electrospin blends of poly(glycerol sebacate) and PCL to control fiber diameter, mechanical properties, and cell attachment [165]. In addition to electrospinning of blends, various innovative electrospinning procedures [166–168], such as microfluidic assisted [169] and *in situ* blending [170,171], have been developed to generate impressive gradient structures with various mechanical properties.

The versatility of electrospinning is not limited to the wide range of materials that can be processed by this method. While at the early stages, electrospinning was mainly used to fabricate thin scaffolds, recently more complex 3D constructs have been developed by altering the geometry of the collecting electrode or spinneret (Fig. 6) [122,172,173]. For instance, various geometries of heart valve leaflets have been prepared by electrospinning of ester-based polyurethane on carefully designed collecting electrodes with insulating and conductive patterns [173]. The 3D geometry of electrodes and their insulating/conductive patterns, along with the deposition time, were the control variables by which artificial valve leaflets replicating native tricuspid, aortic, mitral, and pulmonary valves were produced. This technique allows engineering artificial heart valve with the desirable macroscopic shape and size, mechanical properties, heterogeneity, and microstructure. As shown in Fig. 7, this elegant procedure even enables to engineer suture-free heart valves that integrate the wall scaffolds into valved geometries. Due to the presence of organic solvent and high voltage, cells cannot be directly used in electrospinning; hence, the electrospun scaffolds are used to incorporate desired cells after fabrication. In such after fabrication

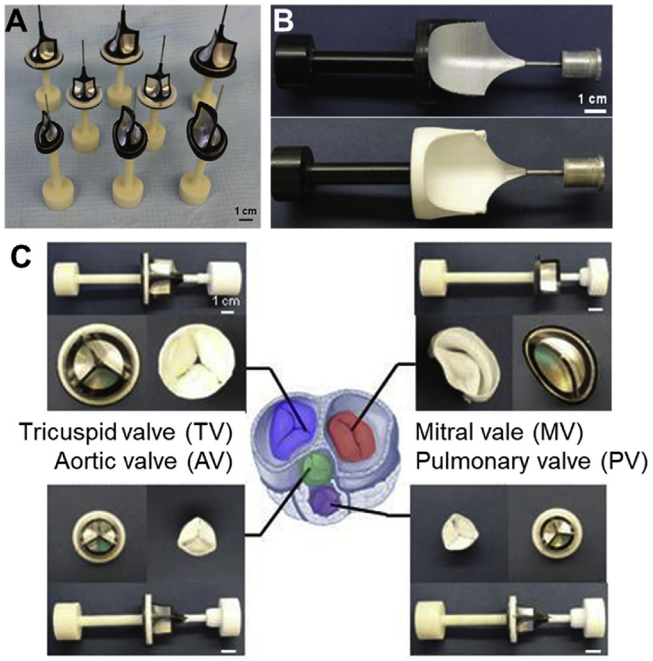

Fig. 7. Electrospinning for the fabrication of heart valves. The geometry of the collector electrodes determines the architecture of the electrospun constructs (A, B) and the type of valves fabricated by electrospinning (C). A variety of such collector electrodes are shown in (A). The collector electrodes may spin during the electrospinning to generate different fiber alignments. An example of a collector electrode after electrospinning is shown in (B). Examples of electrospun tricuspid, aortic, mitral, pulmonary valves are presented in (C). Scale bars are 1 cm. All figures were modified and reprinted with permission from the publisher [173].

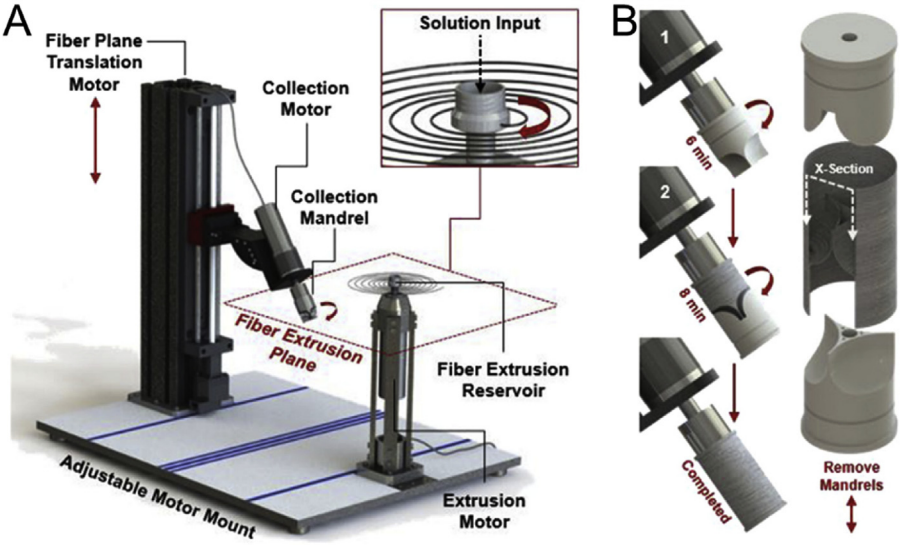

Fig. 6. An example of a modified electrospinning system (JetValve) [122] with a rotary fiber spinning reservoir (A) and customizable collecting electrodes (B) to create more realistic valve geometries via electrospinning.

treatments, cells can be encapsulated in a hydrogel precursor, then applied on the electrospun scaffold [174]. Alternatively, cells are directly seeded on the scaffold in a bioreactor.

4.3. Additive manufacturing

Additive manufacturing has enabled the fabrication of multimaterial structures with complex 3D architectures. From the hardware point of view, 3D printers can easily provide submicron spatial movement, precisely control temperature, and deposit minute amounts of materials at each layer. Yet, to create a finely defined complex and heterogeneous structure, such as that of heart valves, the properties of bioinks must be optimized and tuned according to each specific additive manufacturing technique. Fig. 8A schematically presents the correlation between material properties (e.g. polymer concentration, crosslink density, stiffness) and shape fidelity. In most cases, the materials used for cell culturing have low viscosity and low stiffness, which are suitable conditions for cells but result in shapeless structures. To obtain more defined constructs, on the other hand, it is necessary to use stiffer gels [175]. It must be noted that gels with extremely high stiffness are not compatible with cells. As such, it is highly desirable to achieve well-defined constructs (high fidelity) with soft gels by employing novel biofabrication techniques and new material chemistries. While material development for additive manufacturing is a progressing field, biofabrication has already been demonstrated as an effective tool in biomedical applications and tissue engineering [176]. In the majority of these cases, biofabrication has been used to generate cell-laden scaffolds where cells could be incorporated in the printed structure after the printing or during the course of fabrication [177]. The three common methods of 3D biofabrication are laser-induced forward transfer, inkjet, and extrusion printing (Fig. 8B).

These methods vastly differ from each other, and each entails series of advantages and disadvantages. Inkjet printers require liquid inks with low viscosity (~10 mPa/s). Various types of cells, proteins, and other media can also be incorporated in the inks. While the processing speed and feature resolution are quite high, clogging and other inconsistencies are the major challenges in inkjet printing of customized bioinks. Moreover, inkjet printing cannot be used for the fabrication of 3D structures with large height. This limitation is because inkjet printing can only build features as high as the droplet size, which is in the range of few microns. Extrusion printing can handle a significantly wider range of materials including thermoplastics, hydrogels, gels, and cell-laden media with viscosity varying between 30 mPa/s and 10^2 Pa/s. The processing speed, however, is considerably slower (~5 mm/s) and the feature resolution is poor (normally >50 μm). The laser-induced forward transfer technology uses a donor slide coated with a laser absorbing layer and bioinks containing cells. The coating evaporates when exposed to the laser, releasing a high-pressure gas, which ejects the bioink to the surface. It is a nozzleless process compatible with low-to-medium viscosity inks (1–300 mPa/s). They can also handle cells (up to 10^8 cell/ml) at very high cell viabilities (>95%) [176]. Similar to inkjet printing, laser-induced technologies are not suitable for large constructs and hence are not biologically relevant for widespread applications. Among the common biofabrication techniques, extrusion printing offers considerable flexibility in material design. Hence, the remainder of this section is devoted to this technique and its use in the manufacturing of heart valves and conduits.

Extrusion printing, also referred to as bioplotting in the biological context, is a versatile technique in which the inks – ranging from thermoplastics to gels and highly viscose liquids – are dispensed through a nozzle on a platform [178,179]. The movement of the nozzle or the platform (or both) is fully controlled so that materials are deposited in *x*, *y*, and *z* directions. In most cases, the rate of deposition and temperature of the nozzle and the platform can be controllable. The deposition process is either pneumatic or mechanical, and it is possible to deposit more than one material in each layer [180]. The print resolution is defined by the size of the nozzle and ranges from ~50 μm to a few millimeters. The

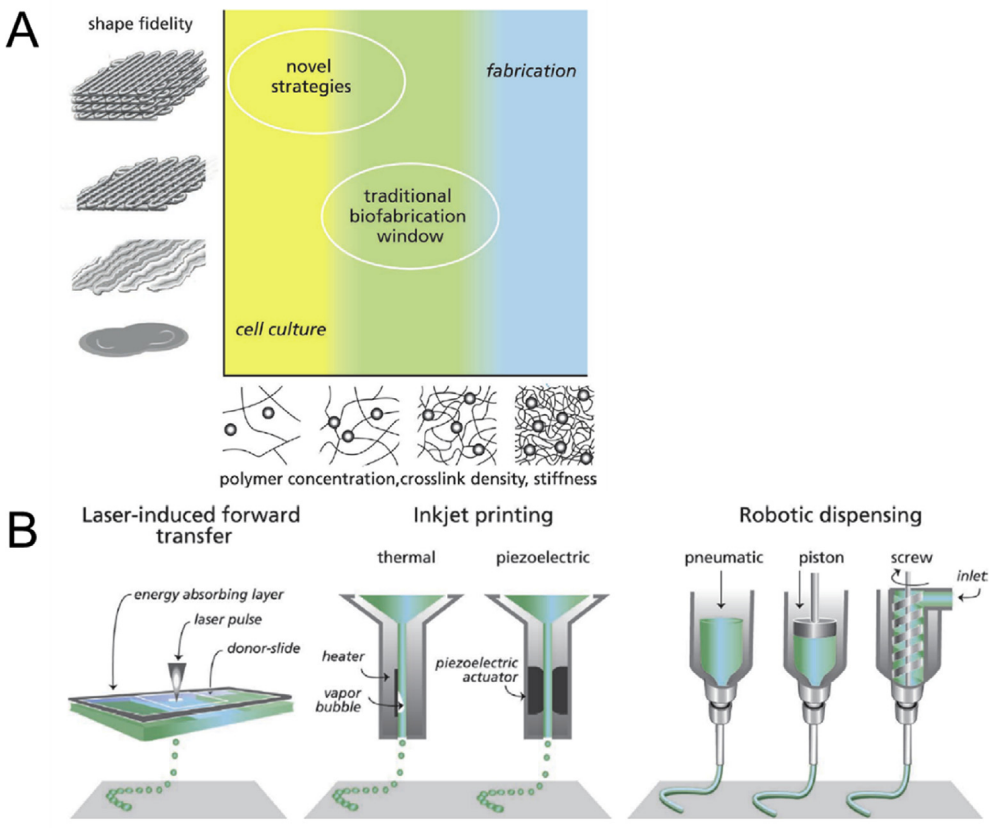

Fig. 8. A schematic representation of shape fidelity as a function of polymer network stiffness (A) [177]. Hydrogels used for cell culturing are not able to retain a predefined geometry while providing a very suitable environment for cells to migrate and grow. On the other hand, stiff hydrogels are highly suitable for the fabrication of well-defined 3D geometries but do not provide an adequate physiological environment for cells. The traditional biofabrication window is where shape fidelity and network stiffness are moderately compromised. Novel strategies are being developed to provide a suitable environment for cells while enabling detailed biofabrication of complex geometries. Common additive manufacturing techniques used in biofabrication of medical devices and scaffolds (B) [177].

main advantages of extrusion printing over other additive manufacturing methods for tissue engineering and medical device fabrication are the ink versatility, stackability, and the possibility of loading high density of cells into the ink [181,182]. The print resolution in extrusion printing, however, is not as high as other methods of 3D printing [183]. Hydrogels are vastly used in extrusion printing of implants as they contain large quantities of water and offer mechanical and physical properties partly matching those of native soft tissues [184]. Common hydrogel-based materials used in ink preparation for extrusion printing include polyethylene glycol (PEG) and polypropylene glycol (PPG) derivatives, alginate [185], gelatin derivatives such as gelatin methacrylate (GelMA) [186,187], agarose [188], collagen [117,189], fibrin [190], silk [191,192], and hyaluronic acid (HA) [193,194].

The wide degrees of freedom in ink design for gel extrusion printing have led to the creation of multimaterial constructs such as 3D vascularized structures [195]. For instance, J.A. Lewis's team used the versatility of extrusion printing to build a 3D construct tissue with multiple cell types, vasculature, and extracellular matrix using a combination of scarifying (Lutrol® F127) and GelMA (cell-laden and pure) inks [196]. A temperature-sensitive copolymer, Lutrol® F127 is routinely used as a support material with gelation temperatures around room temperature (depending on polymer concentration). After gelation, Lutrol® F127 is sufficiently robust to support the mass of other deposited inks, and later can easily be removed by lowering the temperature below the gelation point. GelMA is also a temperature-sensitive biopolymer based on gelatin with polymerizable methacrylate sites. Utilizing thermal gelation of Lutrol® and GelMA, and polymerizability of GelMA, researchers in Lewis's team were able to create multichanneled structures lined with human dermal fibroblasts and human umbilical vein endothelial cells. Cell viability was reported to range from 60% to 80% as expected for extrusion printing. The relatively low cell viability observed in extrusion printing of cell loaded bioinks is attributed to the high shear stress applied to cells during printing. The high shear stress originated from the high viscosity of inks used in extrusion printing can rupture the cell walls. Nair et al. showed that the number of live cells reduces by more than 38% when the maximum shear stress experienced in the fluid increases from ~20 kPa to ~760 kPa [197].

Extrusion printing also allows for printhead modification, to enable *in situ* mixing of inks according to the digital input. Zhang, Khademhosseini, and their colleagues demonstrated the rapid fabrication of multimaterial structures made from several bioinks based on GelMA and alginate using one single printhead [198]. Again, GelMA was used as a polymerizable biopolymer while alginate was a rheological modifier. This method was used in proof-of-concept demonstrations in which patterned endothelialized tissue was fabricated with four bioinks laden with human dermal fibroblasts, HepG2 human hepatocellular cells, human mesenchymal stem cells, and no cells. The main application of *in situ* mixing of multiple inks at the printhead will be in generating structures with gradient composition [199].

The ability of extrusion printing in depositing multimaterials at high throughputs, being compatible with modified printheads, and having a vast library of printable materials, renders this method of additive manufacturing very suitable for the seamless fabrication of artificial heart valves and conduits. The native cardiac valved conduits are highly heterogeneous with complex 3D structures. The cellular heterogeneity of the cardiac valved conduits will be translated into the material heterogeneity in the artificial conduits in order to provide suitable substrates for the inclusion of various cell types [200]. Hockaday et al. [201] used extrusion printing to fabricate aortic valve scaffolds made of polyethylene glycol diacrylate (PEGDA) (Fig. 9).

PEGDA is a polymerizable macromer with two active vinyl groups at each end of its chain, suitable for radical crosslinking. High levels of photoinitiator (Irgacure® 2959) were added to the ink formulation to reduce the crosslinking time to 30–60 s. To achieve heterogeneity in mechanical properties of printed heart valves, Hockaday and colleagues used two types of PEGDA with different chain lengths (i.e. 700 and 8000 Da) and altered their ratio in the inks. PEGDA macromers with shorter chain length lead to stiffer hydrogels. Hence by controlling the ratio of two PEGDAs, the stiffness of hydrogels was tuned between ~5 kPa and ~75 kPa. Alginate was added to the inks (10–15%) as a thickening agent to enable printing, while highly viscose alginate and gelatin ink was used as the support material for overhanging leaflets and ostia. The digital models for the printed aortic valves were based on micro-CT scans of fixed porcine aortic valves, and the printed structures achieved above 90% shape fidelity (10% tolerance) for valved conduits with ID of 22 mm. Yet, the shape fidelity was compromised as the print size reduced. For structures with ID of 12 mm, the shape fidelity was ~70%. After photocrosslinking, alginate and support material were removed from the scaffold, and porcine aortic valve interstitial cells (PAVICs) were seeded. Cell vitality was between 90% and 100% over 21 days but the mean circularity of cells varied with the composition of hydrogel scaffold. While this study demonstrated the feasibility of extrusion printing for the fabrication of heterogeneous cardiac valves using multiple corsslinkable inks, the procedure still requires *in situ* polymerization, hence preventing the inclusion of cells into the inks prior to printing. Consequently, cells were seeded on the scaffold after the printing, which compromises the heterogeneity of the construct as only one cell type could be used. To enable direct cell-hydrogel printing, cells must be encapsulated to obtain high cell vitality [202].

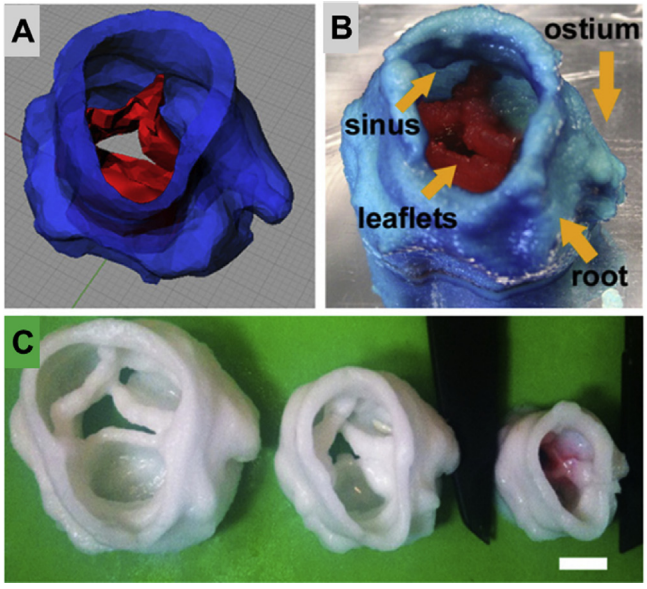

Fig. 9. 3D printing of multimaterial heart valves: a 3D model is used (A) as a feed for the printer to construct an aortic heart valves (B). The 3D printing allows for rescaling of the printed constructs (C) for better customization. The scale bar in (C) is 1 cm. All figures were modified and reprinted with permission from the publisher [201].

To eliminate the harsh chemical environment that arises from the polymerization of low viscose inks, physically crosslinkable biopolymers with thermal gelation, such as gelatin, have been proposed for direct cell printing of cardiac valves. For instance, aortic root sinus smooth muscle cells (SMC) and aortic valve leaflet interstitial cells (VIC) were separately mixed with a temperature-sensitive ink comprised of alginate and gelatin (2×10^6 cells/ml) then printed into aortic valve constructs [125]. Gelation took place by reducing the ink temperature from 37 °C to room temperature, followed by immersion in $CaCl_2$ for further ionic crosslinking of alginate. The cell viability of both cell types was more than 80% within the 3D printed tissues and encapsulated VIC expressed elevated vimentin while SMC expressed elevated alpha-smooth muscle actin (α-SMA). It was found that incorporation of cells into the inks reduced the ultimate strength, stiffness, and maximum elongation of the hydrogels. By incubating the hydrogels (with or without cells), their

mechanical properties deteriorated over time, which can be due to the physically crosslinked nature of the hydrogels.

Methacrylated biopolymers with thermal gelation can also be used for cell printing to take advantage of their thermal gelation immediately after printing followed by covalent crosslinking to obtain more robust constructs. Human aortic valvular interstitial cells (HAVIC) were encapsulated in methacrylated hyaluronic acid (MA-HA) and GelMA for 3D printing of a trileaflet valve shape [203]. Since the thermal gelation immediately after printing led to a stable 3D structure, it was possible to use lower levels of photoinitiator (i.e. 0.05% of Irgacure® 2959) at the expense of prolonged UV irradiation (~ 5 min). The mild radical crosslinking reaction resulted in cell viability above 90%, while the stiffness of the hydrogel construct and the rheology of the inks prior to printing were controlled by adjusting the ratio of MA-HA and GelMA. After 7 days of incubation, the encapsulated HAVIC expressed both α-SMA and vimentin, indicating the activation of HAVIC from fibroblastic to myofibroblastic. To better control the mechanical properties of the methacrylated biopolymers, additional crosslinkers, such as polyethylene glycol diacrylate, may be added to the formulation of the inks [204]. Addition of crosslinkers can reduce the level of initiator and time and dose of irradiation needed to achieve a hydrogel scaffold with adequate mechanical stability.

An emerging strategy to create tissue-specific bioinks is by utilizing the decellularized extracellular matrix (dECM) [206] as the base for the ink to which various forms of biopolymers or synthetic polymers, rheology modifiers, and different cell types can be added (Fig. 10) [205,207,208]. In one study, cardiomyocytes were added to the dECM extracted from the left ventricle of a pig to prepare a temperature-sensitive bioink. To enable photocrosslinking, vitamin B2 was also added to the ink ECM formulation as a photoinitiator [209]. After printing, the scaffold was initially gelled by UVA light followed by incubation at 37 °C. Self-supporting cells were also printed into cardiac tubes with the aid of a suitable support material [210]. However, achieving higher degrees of structural complexity might not be possible with this approach because of the inadequate rheological properties of cell-only inks.

5. Challenges and perspectives

Heart valves have extremely anisotropic mechanical properties, which originate from their heterogeneous structure at various scales. Hence, there is no single category of artificial heart valves that could address all mechanical requirements of heart valves (Table 4). Therefore, despite all advances in materials science and manufacturing, so far only mechanical and bioprosthetic heart valves have been used clinically.

The reported values for mechanical properties of the bovine pericardium and porcine pericardium, which are often used as bioprosthetic heart valves, are inconsistent in the literature. However, it can be inferred that adult bovine pericardium and calf bovine pericardium were significantly stiffer than fetal bovine pericardium. The porcine pericardium has been found thinner and stiffer than bovine pericardium. It should be noted that no significant difference has been reported between the tensile properties of GT-KO and wild-tissue [66].

Table 4
Advantages and challenges of various types of heart valves.

Valve-type	Advantages	Disadvantages
Mechanical	- Durability - Ease of fabrication with robust mechanical properties	- Durability, blood clotting due to high shear stress
Biological	- Close resemblance to native tissues	- Durability and lack of customization
Polymeric	- Processable via novel fabrication techniques such as additive manufacturing and electrospinning, which allow for customization and creation of complex geometries - Mechanical properties resemble those of native tissues	- Durability and poor dynamic mechanical properties

Gauging the mechanical properties of various materials against native heart valve tissues suggests that many classes of materials can indeed surpass the *static* mechanical properties of heart tissues. Yet, this oversimplified comparison is highly misleading. Indeed, the majority of such materials fail to maintain their desirable mechanical properties under the demanding dynamic conditions in which heart valves operate. Fig. 11 presents a comparison between modulus (E_e: elastin region, E_c: collagen region), strain at break (ε_b), ultimate strength (σ_b), and fracture energy (G) of various materials and heart valve tissues. For better clarification, all properties have been normalized to those of aortic wall in the axial direction at the root of the aortic valve.

Simple hydrogels, such as covalently crosslinked PAAm [113] or ionically crosslinked alginate [137], fail to offer adequate modulus, strength, or toughness. Tough hydrogels, such as DN [211] or hybrid [137] hydrogels, have considerably higher toughness and strain at break than heart tissues with comparable strength. However, their modulus (~0.1–1 MPa) is lower than the circumferential modulus of heart tissues in the collagen phase (Fig. 11A). On the other hand, elastomers such as Lubrizol [78], SIBS [101], and P4HB [107], as well as PTFE [90,91,212], offer considerably higher mechanical properties compared to hydrogels and native heart tissues (Fig. 11B).

For better highlighting the complexity of material design for heart valves, Fig. 12 compares the tensile mechanical properties of various materials that have been used for heart valve applications against native heart tissues. In Fig. 12, the mechanical properties of heart tissues span over a wide range, which reflects their anisotropic behavior. Again,

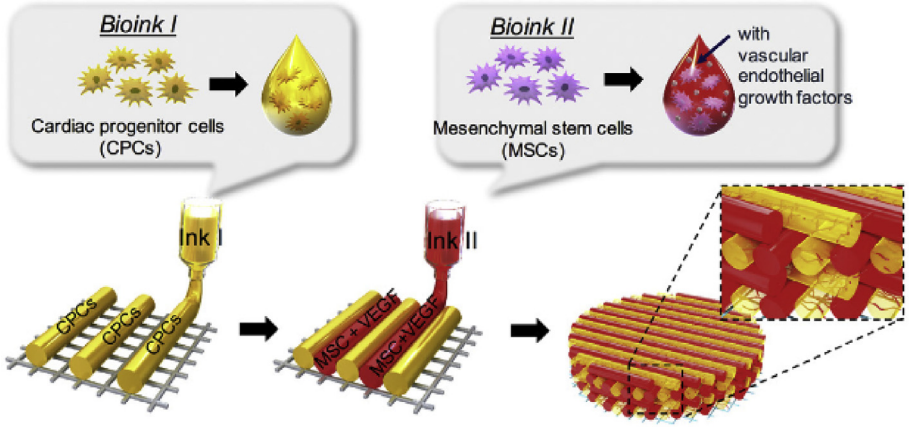

Fig. 10. Customizing bioinks by incorporating various cell types into dECM. All figures were modified and reprinted with permission from the publisher [205].

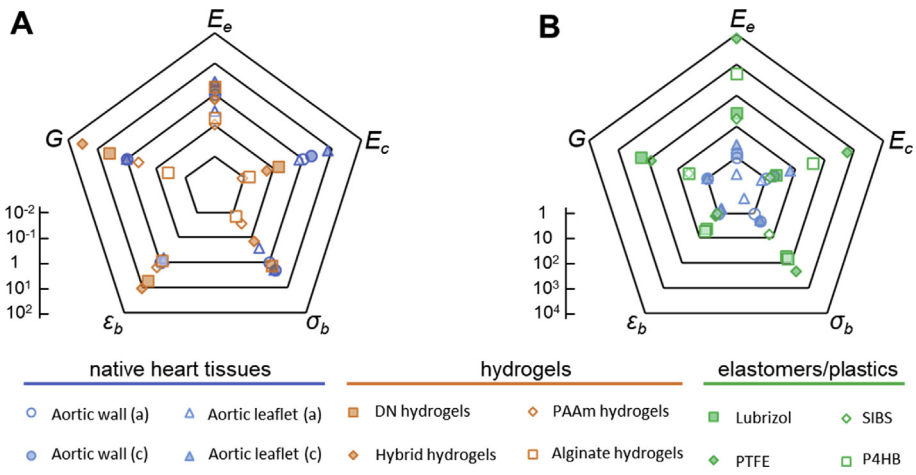

Fig. 11. Comparing mechanical properties of hydrogels (A) and elastomers/plastics (B) with those of native heart tissues. The data points represent tensile modulus (E), tensile strength (σ_b), tensile strain at break (ε_b), and fracture energy (G) normalized to properties of the aortic wall in axial direction (logarithmic scale). *a*: axial, *c*: circumferential, *r*: radial, E_e: modulus of elastin region, E_c: modulus of collagen region. For aortic wall (a): E_e = 140 kPa, E_c = 1.72 MPa, σ_b = 720 kPa, ε_b = 86%, and G = 250 J m^{-2}.

elastomers such as PU and PHA exhibit superior mechanical properties compared to soft materials such as fibrins and collagen-based scaffolds. The static mechanical data such as those used to construct Figs. 11 and 12, however, must be handled with caution. Indeed, any potential material that is being considered for the fabrication of new heart valves must be able to withstand long-term dynamic deformations under biological conditions. Hence, the combination of high toughness, strain at break, and strength only points to potential suitability of such materials.

It should be highlighted that the tensile properties such as Young's elastic modulus (E) are related to the bending properties, that is, flexural stiffness (κ) as follows [219]:

$$\kappa = EI \tag{1}$$

where 'I' is the moment of inertia. For a simple beam, the flexural stiffness would be:

$$\kappa = E\frac{wh^3}{12} \tag{2}$$

in which 'w' and 'h' are width and thickness of the material. For soft materials, Young's modulus is small, which results in a subsequently small κ. Hence, to reach a desired flexural stiffness, thicker materials would be required. In contrast, for rigid materials with higher modulus, the valve should be constructed thinner to provide the same flexural stiffness. Making extremely thin valve leaflets could be a challenge in manufacturing and may also introduce more defects. Hence, understanding the tensile properties of the constituent materials of the artificial heart valve is essential for manufacturing. The flexural properties can also be directly determined through three-point bending [220], cantilever bending [221], and microindentation [222], and their measurements would be beneficial to predict the flexural performance of the engineered heart valve.

The continuous cyclic stress applied to the heart valves caused by stretching, bending, and shear is the main source of mechanical fatigue and failure in artificial heart valves. Thus, significant attention must be paid to long-term viscoelastic and fatigue properties of materials used in engineered heart valves. As discussed earlier, the mechanical properties of heart valves are not the same in all directions (e.g. circumferential versus radial). Martin et al. [223] demonstrated that by applying a high number of load/unload cycles on native heart valve tissues, the strain rate dependence decreased in both circumferential (Fig. 13A) and radial (Fig. 13B) directions. In other words, the viscous effects disappeared while the non-linear elasticity remained [223]. Such viscoelastic properties may be found in synthetic elastomers such as thermoplastic polyurethanes (Fig. 13C) [224], or even in some novel tough hydrogels (Fig. 13D) [137]. Nevertheless, there is no non-biological material that could replace the self-healing trait for native heart valves.

To better design and engineer an artificial heart valve, it is essential to understand the complex stress regime that will be applied to it. In this domain, computational modeling is the only available analytical tool. Specifically, the fluid–structure interaction models can be extremely useful in the design and evaluating the mechanical performance of artificial heart valves (Fig. 14) [225,226]. These models can predict the valve closure and mechanical deformation of the valves under simulated hemodynamic conditions. The mechanical properties of the suggested materials and various valvular designs could be used as inputs for these

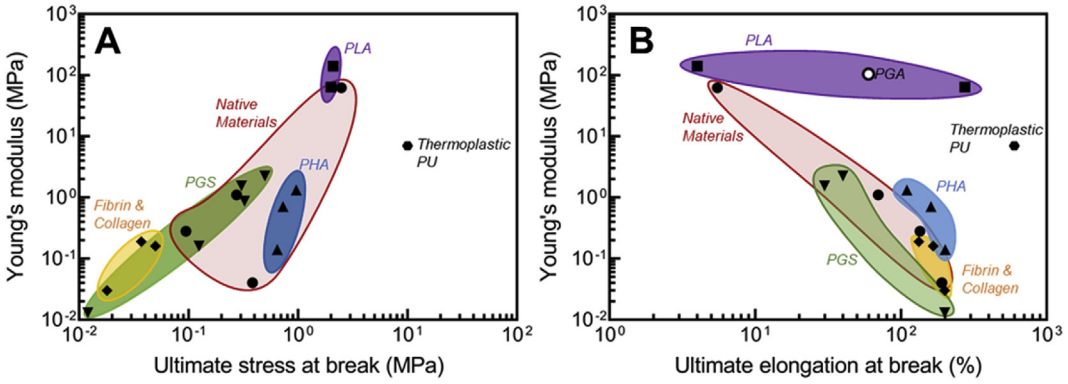

Fig. 12. Mechanical properties of various materials (e.g. native valves [142,172,213], PLA [172], PHA [142], PGS [213,214], fibrin and collagen [215,216], electrospun PGA [217], and thermoplastic PU [218]) used in fabrication of polymeric heart valves: Young's modulus versus ultimate stress at break (A) and Young's modulus versus elongation at break (B).

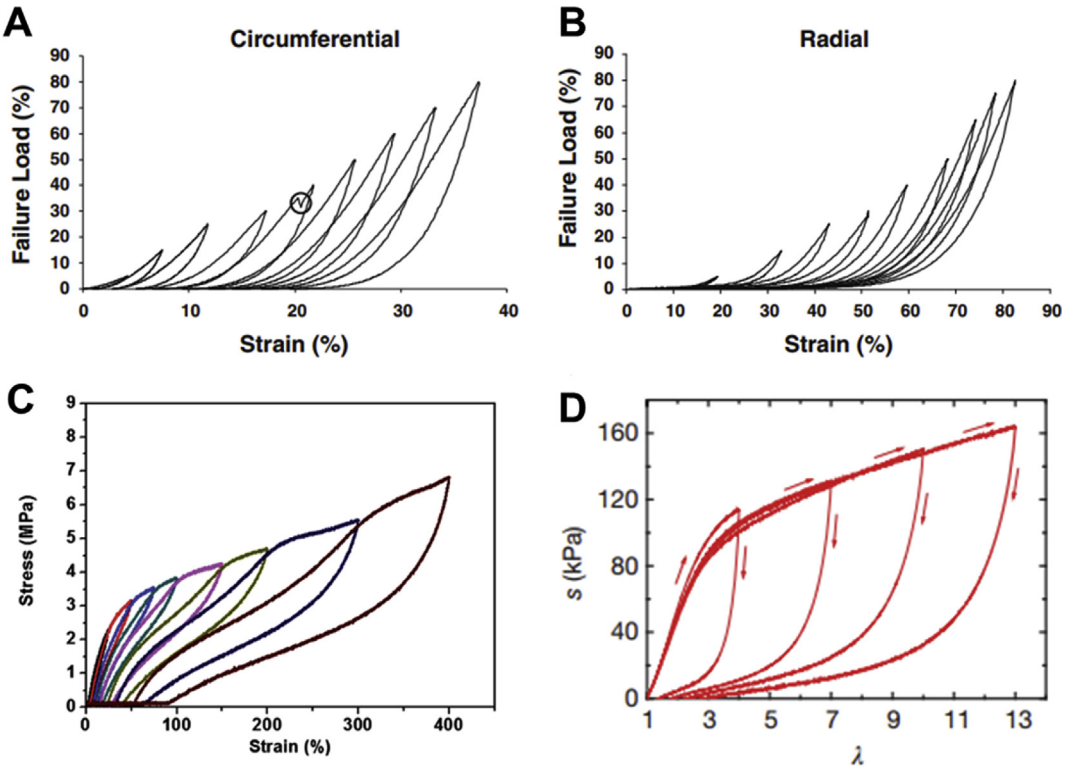

Fig. 13. Cyclic load/unload performance of native heart valve in circumferential (A) and radial (B) directions [223]. The cyclic behavior of (C) thermoplastic polyurethane [224] and (D) a tough hybrid hydrogel [137]. All figures were reprinted with permission from the publishers.

models. The simulation then will aid the researchers and engineers in assessing the performance of the artificial heart valves before *in vivo* studies.

It is also important to note that healthy heart tissues can recover at the molecular level. Most synthetic materials, on the other hand, do not exhibit any mechanism for recovery, meaning that after extreme deformation, their performance may deteriorate beyond repair. The recent advancements in developing materials, such as crosslinked hydrogels, with dynamic interchain bonding may assist in addressing the need for recovery of synthetic materials after deformation. Such self-healing materials benefit from one or more types of dynamic bondings such as hydrogen bonds [227–229], ionic interactions [137,230], or hydrophobic interactions [231]. Yet, many fundamental questions still remain to be addressed to enable employing self-healing materials for heart valve applications. For instance, the rate of recovery must be comparable with the deformation induced in the material.

Very recently, Xeltis has made promising advances in developing a completely polymer-based platform (RestoreX) for the restoration of

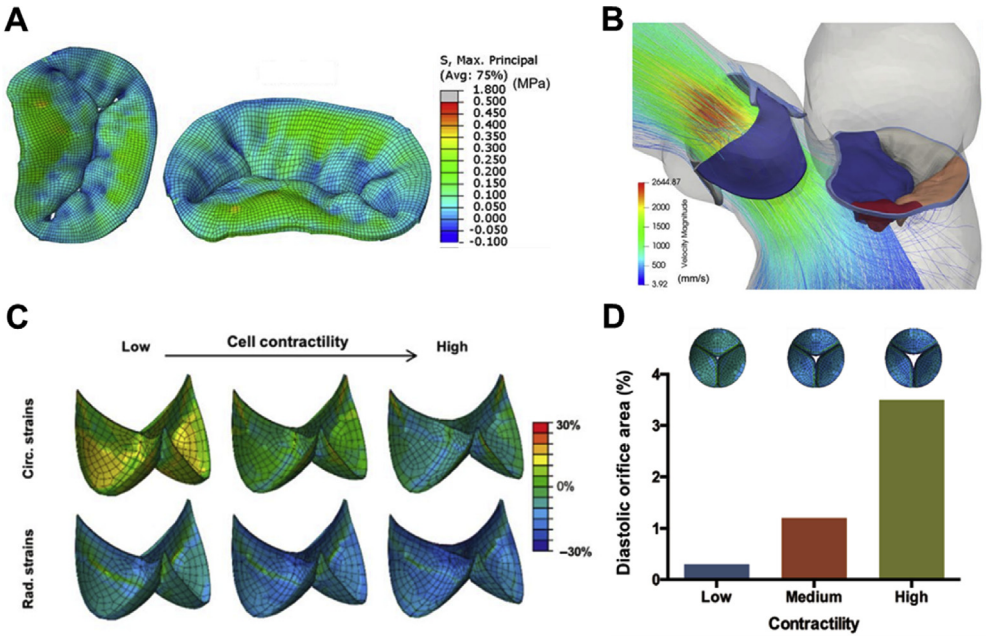

Fig. 14. Computational modeling of heart valves. Stress distribution in the mitral leaflets at peak systole (A) [225], velocity streamlines in the mitral valve at peak systole (B) [225], circumferential and radial strains in the loaded configuration in a tissue-engineered pulmonary valve upon variations in cell contractility (C) [226], and the predicted valve closure in diastole as a function of contractility (D) [226]. The simulations were performed using the commercial finite-element package Abaqus/Explicit. All figures were reprinted with permission from the publishers.

endogenous tissue using electrospun bioabsorbable bis-urea modified polycarbonate [145]. This technology conceptually relies on the regrowth of tissue through the fibrous structure of the bioabsorbable implant to eventually replace the valved conduit altogether. The implanted valves will initially have adequate mechanical properties to function as an artificial valve but will degrade over time while the tissue is growing through the construct. Through a small-scale clinical trial on pediatric patients, the Xeltis team were able to demonstrate the safety and 12-month survival rate of the subjects. Further clinical studies aim to test the efficacy and device failure rate in both short- and long-term, and the outcomes are yet to be released.

Most materials used for heart valves in preclinical studies were fabricated by either casting or electrospinning (see Table 3). While additive manufacturing such as 3D printing promises ample opportunities, still there are several challenges to prepare this method of fabrication for preclinical studies. The stackability of most bioinks for complex geometries such as a heart valve is still not great and demands more studies. On the other hand, the ability to print various types of cells while printing the scaffolds can provide multiple degrees of freedom for engineering the scaffold with certain cells. Additionally, additive manufacturing of heart valves will offer the opportunity of fabricating patient-specific heart valves. In principle, additive manufacturing is better suited for generating heterogeneous constructs compared to molding and electrospinning. The layer-by-layer nature of additive manufacturing can assist in creating highly anisotropic structures by 3D printing different materials at each layer and controlling the direction of printing, which will resemble the overall multilayered architecture of heart valves. For this purpose, the rheological properties of bioinks must be finely tuned to enable 3D fabrication of valve constructs at high resolutions.

6. Conclusions

There is an urgent need for developing alternative heart valves to overcome long-term stability and biocompatibility issues that are associated with artificial heart valves. This review demonstrates that while a broad range of materials and fabrication technologies have been developed and attempted for designing novel artificial heart valves, this field is still underdeveloped. Currently, the main clinical treatments are still limited to the mechanical and bioprosthetic valves. While there are many categories of polymeric materials with 'static' mechanical properties exceeding those of native heart tissues, very few polymeric, artificial valves, such as RestorX by Xeltis, have reached pre-clinical trials. The slow progress in this area is the results of valves' highly demanding mechanical and biological requirements, the complex and anisotropic geometries of valves, and the lack of self-recovery in artificial materials. In the light of recent progresses made in materials sciences, particularly tough and processable hydrogels, it is anticipated that in future various inks can be designed to take advantage of additive manufacturing to construct personalized heart valve with anisotropic properties. Innovative electrospinning methods can also be utilized to create highly complex and hybrid constructs resembling the geometry of heart valves. Nevertheless, the main challenge faced by material engineers will be to create new, processable, self-healing materials that can offer adequate mechanical properties for highly 'dynamic' biological environments. While various self-healing materials have been developed, none so far have been used for fabrication of heart valves. Moreover, in the case of congenital heart disease, it would be ideal to create a construct that enables size adoption to minimize the number of surgical operations for young patients.

Declaration of competing interest

The authors declare that they have no known competing financial interests or personal relationships that could have appeared to influence the work reported in this article.

Acknowledgements

The authors acknowledge the financial support from the Australian Research Council, the University of Sydney and the Sydney Children Hospital Network. F.O. acknowledges the support of FH Loxton Post-doctoral Fellowship within the University of Sydney.

References

[1] J.K. Williams, J.J. Yoo, A. Atala, Regenerative medicine approaches for tissue engineered heart valves, in: Principles of Regenerative Medicine, Elsevier, 2019, pp. 1041–1058.
[2] G. Thanassoulis, C.Y. Campbell, D.S. Owens, J.G. Smith, A.V. Smith, G.M. Peloso, K.F. Kerr, S. Pechlivanis, M.J. Budoff, T.B. Harris, Genetic associations with valvular calcification and aortic stenosis, N. Eng. J. Med. 368 (2013) 503–512, https://doi.org/10.1056/NEJMoa1109034.
[3] A. Saurav, V.M. Alla, M. Kaushik, C.C. Hunter, A.V. Mooss, Outcomes of mitral valve repair compared with replacement in patients undergoing concomitant aortic valve surgery: a meta-analysis of observational studies, Eur. J. Cardiothorac. Surg. 48 (2014) 347–353, https://doi.org/10.1093/ejcts/ezu421.
[4] E.S. Fioretta, P.E. Dijkman, M.Y. Emmert, S.P. Hoerstrup, The future of heart valve replacement: recent developments and translational challenges for heart valve tissue engineering, J. Tissue Eng. Regenerat. Med. 12 (2018) e323–e335, https://doi.org/10.1002/term.2326.
[5] M. Yacoub, J. Takkenberg, Will heart valve tissue engineering change the world? Nat. Rev. Cardiol. 2 (2005) 60, https://doi.org/10.1038/ncpcardio0112.
[6] M.Y. Emmert, S.P. Hoerstrup, Regenerative transcatheter valves, Eur. Heart J. 38 (2017) 2710–2713, https://doi.org/10.1093/eurheartj/ehx476.
[7] E. Fioretta, L. von Boehmer, S. Motta, V. Lintas, S. Hoerstrup, M. Emmert, Cardiovascular tissue engineering: from basic science to clinical application, Exp. Gerontol. 117 (2019) 1–12, https://doi.org/10.1016/j.exger.2018.03.022.
[8] D.P. Kenny, Z.M. Hijazi, Current status and future potential of transcatheter interventions in congenital heart disease, Circ. Res. 120 (2017) 1015–1026, https://doi.org/10.1161/circresaha.116.309185.
[9] T.C. Flanagan, J.S. Sachweh, J. Frese, H. Schnöring, N. Gronloh, S. Koch, R.H. Tolba, T. Schmitz-Rode, S. Jockenhoevel, In vivo remodeling and structural characterization of fibrin-based tissue-engineered heart valves in the adult sheep model, Tissue Eng. A 15 (2009) 2965–2976, https://doi.org/10.1089/ten.tea.2009.0018.
[10] B. Weber, J. Scherman, M.Y. Emmert, J. Gruenenfelder, R. Verbeek, M. Bracher, M. Black, J. Kortsmit, T. Franz, R. Schoenauer, Injectable living marrow stromal cell-based autologous tissue engineered heart valves: first experiences with a one-step intervention in primates, Eur. Heart J. 32 (2011) 2830–2840, https://doi.org/10.1093/eurheartj/ehr059.
[11] J. Reimer, Z. Syedain, B. Haynie, M. Lahti, J. Berry, R. Tranquillo, Implantation of a tissue-engineered tubular heart valve in growing lambs, Ann. Biomed. Eng. 45 (2017) 439–451, https://doi.org/10.1007/s10439-016-1605-7.
[12] A. Driessen-Mol, M.Y. Emmert, P.E. Dijkman, L. Frese, B. Sanders, B. Weber, N. Cesarovic, M. Sidler, J. Leenders, R. Jenni, Transcatheter implantation of homologous "off-the-shelf" tissue-engineered heart valves with self-repair capacity: long-term functionality and rapid in vivo remodeling in sheep, J. Am. Coll. Cardiol. 63 (2014) 1320–1329, https://doi.org/10.1016/j.jacc.2013.09.082.
[13] C.E. Eckert, B.T. Mikulis, D. Gottlieb, D. Gerneke, I. LeGrice, R.F. Padera, J.E. Mayer, F.J. Schoen, M.S. Sacks, Three-dimensional quantitative micromorphology of pre-and post-implanted engineered heart valve tissues, Ann. Biomed. Eng. 39 (2011) 205–222, https://doi.org/10.1007/s10439-010-0162-8.
[14] Y.S. Zhang, K. Yue, J. Aleman, K. Mollazadeh-Moghaddam, S.M. Bakht, J. Yang, W. Jia, V. Dell'Erba, P. Assawes, S.R. Shin, 3D bioprinting for tissue and organ fabrication, Ann. Biomed. Eng. 45 (2017) 148–163, https://doi.org/10.1007/s10439-016-1612-8.
[15] C.V. Bouten, A.I. Smits, F.P. Baaijens, Can we grow valves inside the heart? Perspective on material-based in situ heart valve tissue engineering, Front. Cardiovasc. Med. 5 (2018), https://doi.org/10.3389/fcvm.2018.00054.
[16] A. Franzone, R. Piccolo, G.C. Siontis, J. Lanz, S. Stortecky, F. Praz, E. Roost, R. Vollenbroich, S. Windecker, T. Pilgrim, Transcatheter aortic valve replacement for the treatment of pure native aortic valve regurgitation: a systematic review, JACC Cardiovasc. Interv. 9 (2016) 2308–2317, https://doi.org/10.1016/j.jcin.2016.08.049.
[17] S. Westaby, R.B. Karp, E.H. Blackstone, S.P. Bishop, Adult human valve dimensions and their surgical significance, Am. J. Cardiol. 53 (1984) 552–556, https://doi.org/10.1016/0002-9149(84)90029-8.
[18] M. Daimon, G. Saracino, A.M. Gillinov, Y. Koyama, S. Fukuda, J. Kwan, J.M. Song, V. Kongsaerepong, D.A. Agler, J.D. Thomas, Local dysfunction and asymmetrical deformation of mitral annular geometry in ischemic mitral regurgitation: a novel computerized 3D echocardiographic analysis, Echocardiog 25 (2008) 414–423, https://doi.org/10.1111/j.1540-8175.2007.00600.x.
[19] A. Hasan, K. Ragaert, W. Swieszkowski, Š. Selimović, A. Paul, G. Camci-Unal, M.R. Mofrad, A. Khademhosseini, Biomechanical properties of native and tissue engineered heart valve constructs, J. Biomech. 47 (2014) 1949–1963, https://doi.org/10.1016/j.jbiomech.2013.09.023.
[20] X. Shen, L. Bai, L. Cai, X. Cao, A geometric model for the human pulmonary valve in its fully open case, PLoS One 13 (2018), e0199390, https://doi.org/10.1371/journal.pone.0199390.

[21] D.Y. Cheung, B. Duan, J.T. Butcher, Current progress in tissue engineering of heart valves: multiscale problems, multiscale solutions, Expert Opin. Biol. Ther. 15 (2015) 1155–1172, https://doi.org/10.1517/14712598.2015.1051527.

[22] M.S. Sacks, A.P. Yoganathan, Heart valve function: a biomechanical perspective, Philos. Trans. Royal Soc. B 362 (2007) 1369–1391, https://doi.org/10.1098/rstb.2007.2122.

[23] K.J. Grande-Allen, J. Liao, The heterogeneous biomechanics and mechanobiology of the mitral valve: implications for tissue engineering, Curr. Cardiol. Rep. 13 (2011) 113–120, https://doi.org/10.1007/s11886-010-0161-2.

[24] P. Stradins, R. Lacis, I. Ozolanta, B. Purina, V. Ose, L. Feldmane, V. Kasyanov, Comparison of biomechanical and structural properties between human aortic and pulmonary valve, Eur. J. Cardiothorac. Surg. 26 (2004) 634–639, https://doi.org/10.1016/j.ejcts.2004.05.043.

[25] A. Desai, T. Vafaee, P. Rooney, J.N. Kearney, H.E. Berry, E. Ingham, J. Fisher, L.M. Jennings, In vitro biomechanical and hydrodynamic characterisation of decellularised human pulmonary and aortic roots, J. Mech. Behav. Biomed. Mater. 79 (2018) 53–63, https://doi.org/10.1016/j.jmbbm.2017.09.019.

[26] F.M. Filipoiu, The structure of the heart, in: Atlas of Heart Anatomy and Development, Springer London, London, 2014, pp. 151–201.

[27] I. Vesely, Heart valve tissue engineering, Circ. Res. 97 (2005) 743–755, https://doi.org/10.1161/01.RES.0000185326.04010.9f.

[28] M.S. Sacks, W. David Merryman, D.E. Schmidt, On the biomechanics of heart valve function, J. Biomech. 42 (2009) 1804–1824, https://doi.org/10.1016/j.jbiomech.2009.05.015.

[29] W.D. Merryman, I. Youn, H.D. Lukoff, P.M. Krueger, F. Guilak, R.A. Hopkins, M.S. Sacks, Correlation between heart valve interstitial cell stiffness and transvalvular pressure: implications for collagen biosynthesis, Am. J. Physiol. Heart Circ. Physiol. 290 (2006) H224–H231, https://doi.org/10.1152/ajpheart.00521, 2005.

[30] J.T. Butcher, G.J. Mahler, L.A. Hockaday, Aortic valve disease and treatment: the need for naturally engineered solutions, Adv. Drug Deliv. Rev. 63 (2011) 242–268, https://doi.org/10.1016/j.addr.2011.01.008.

[31] M. Thubrikar, W.C. Piepgrass, J.D. Deck, S.P. Nolan, Stresses of natural versus prosthetic aortic valve leaflets in vivo, Ann. Thorac. Surg. 30 (1980) 230–239, https://doi.org/10.1016/S0003-4975(10)61250-7.

[32] J.M. Lee, D.W. Courtman, D.R. Boughner, The glutaraldehyde-stabilized porcine aortic valve xenograft. I. Tensile viscoelastic properties of the fresh leaflet material, J. Biomed. Mater. Res. 18 (1984) 61–77, https://doi.org/10.1002/jbm.820180108.

[33] P. Dagum, G.R. Green, F.J. Nistal, G.T. Daughters, T.A. Timek, L.E. Foppiano, A.F. Bolger, N.B. Ingels, D.C. Miller, Deformational dynamics of the aortic root, Circulation 100 (1999) II54–62, https://doi.org/10.1161/01.cir.100.suppl_2.ii-54.

[34] Y.F. Missirlis, C.D. Armeniades, Stress analysis of the aortic valve during diastole: important parameters, J. Biomech. 9 (1976) 477–480, https://doi.org/10.1016/0021-9290(76)90091-9.

[35] N.S. Chahal, M. Drakopoulou, A.M. Gonzalez-Gonzalez, R. Manivarmane, R. Khattar, R. Senior, Resting aortic valve area at normal transaortic flow rate reflects true valve area in suspected low-gradient severe aortic stenosis, JACC Cardiovasc. Imaging 8 (2015) 1133–1139, https://doi.org/10.1016/j.jcmg.2015.04.021.

[36] K. Balachandran, P. Sucosky, A.P. Yoganathan, Hemodynamics and mechanobiology of aortic valve inflammation and calcification, Int. J. Inflamm. 2011 (2011), https://doi.org/10.4061/2011/263870.

[37] C.H. Yap, N. Saikrishnan, G. Tamilselvan, A.P. Yoganathan, Experimental measurement of dynamic fluid shear stress on the aortic surface of the aortic valve leaflet, Biomechanics Model. Mechanobiol. 11 (2012) 171–182, https://doi.org/10.1007/s10237-011-0301-7.

[38] I.A. Jawad, M.H. Ghali, R.L. Brown, Y.H. Sohn, Pressure-flow relations across the normal mitral valve, Am. J. Cardiol. 59 (1987) 915–918, https://doi.org/10.1016/0002-9149(87)91119-2.

[39] J. Lee, Z. Estlack, H. Somaweera, X. Wang, C.M. Lacerda, J. Kim, A microfluidic cardiac flow profile generator for studying the effect of shear stress on valvular endothelial cells, Lab Chip 18 (2018) 2946–2954, https://doi.org/10.1039/C8LC00545A.

[40] D. Du, S. Jiang, Z. Wang, Y. Hu, Z. He, Effects of suture position on left ventricular fluid mechanics under mitral valve edge-to-edge repair, Bio Med. Mater. Eng. 24 (2014) 155–161, https://doi.org/10.1007/s13239-010-0022-6.

[41] M.M. Bissell, M. Loudon, S. Neubauer, S.G. Myerson, Abnormal haemodynamic flow patterns in bicuspid pulmonary valve disease, Front. Physiol. 8 (2017) 374, https://doi.org/10.3389/fphys.2017.00374.

[42] N.B. Karatzas, G.D.E.J. Lee, Propagation of blood flow pulse in the normal human pulmonary arterial system: analysis of the pulsatile capillary flow, Circ. Res. 25 (1969) 11–21, https://doi.org/10.1161/01.res.25.1.11.

[43] V. Danicek, A. Sagie, M. Vaturi, D.E. Weisenberg, G. Rot, Y. Shapira, Relation of tricuspid inflow E-wave peak velocity to severity of tricuspid regurgitation, Am. J. Cardiol. 98 (2006) 399–401, https://doi.org/10.1016/j.amjcard.2006.02.045.

[44] V.L. Gott, D.E. Alejo, D.E. Cameron, Mechanical heart valves: 50 years of evolution, Ann. Thorac. Surg. 76 (2003) S2230–S2239, https://doi.org/10.1016/j.athoracsur.2003.09.002.

[45] J.S. Swanson, A. Starr, The ball valve experience over three decades, Ann. Thorac. Surg. 48 (1989) S51–S52, https://doi.org/10.1016/0003-4975(89)90636-X.

[46] R.O. Ritchie, R.H. Dauskardt, W. Yu, A.M. Brendzel, Cyclic fatigue-crack propagation, stress-corrosion, and fracture-toughness behavior in pyrolytic carbon-coated graphite for prosthetic heart valve applications, J. Biomed. Mater. Res. 24 (1990) 189–206, https://doi.org/10.1002/jbm.820240206.

[47] F.J. Schoen, On the fatigue behavior of pyrolytic carbon, Carbon 11 (1973) 413–IN420, https://doi.org/10.1016/0008-6223(73)90081-X.

[48] L. Ma, G. Sines, Fatigue behavior of a pyrolytic carbon, J. Biomed. Mater. Res. 51 (2000) 61–68, https://doi.org/10.1002/(SICI)1097-4636(200007)51:1<61::AID-JBM9>3.0.CO;2-Z.

[49] R.O. Ritchie, R.H. Dauskardt, F.J. Pennisi, On the fractography of overload, stress corrosion, and cyclic fatigue failures in pyrolytic-carbon materials used in prosthetic heart-valve devices, J. Biomed. Mater. Res. 26 (1992) 69–76, https://doi.org/10.1002/jbm.820260107.

[50] M. Sakai, R.C. Bradt, D.B. Fischbach, Fracture toughness anisotropy of a pyrolytic carbon, J. Mater. Sci. 21 (1986) 1491–1501, https://doi.org/10.1007/bf01114701.

[51] J.J. Kruzic, S.J. Kuskowski, R.O. Ritchie, Simple and accurate fracture toughness testing methods for pyrolytic carbon/graphite composites used in heart-valve prostheses, J. Biomed. Mater. Res. 74A (2005) 461–464, https://doi.org/10.1002/jbm.a.30380.

[52] D. Mavrilas, Y. Missirlis, An approach to the optimization of preparation of bioprosthetic heart valves, J. Biomech. 24 (1991) 331–339, https://doi.org/10.1016/0021-9290(91)90351-M.

[53] C. Harris, B. Croce, C. Cao, Tissue and mechanical heart valves, Ann. Cardiothorac. Surg. 4 (2015), https://doi.org/10.3978/j.issn.2225-319X.2015.07.01, 399–399.

[54] R. D'souza, J. Ostro, P.S. Shah, C.K. Silversides, A. Malinowski, K.E. Murphy, M. Sermer, N. Shehata, Anticoagulation for pregnant women with mechanical heart valves: a systematic review and meta-analysis, Eur. Heart J. 38 (2017) 1509–1516, https://doi.org/10.1093/eurheartj/ehx032.

[55] C. Armeniades, L. Lake, Y. Missirlis, J. Kennedy, Histologic origin of aortic tissue mechanics: the role of collagenous and elastic structures, Appl. Polym. Symp. 22 (1973) 319–339.

[56] R. Clark, Stress-strain characteristics of fresh and frozen human aortic and mitral leaflets and chordae tendineae. Implications for clinical use, J. Thorac. Cardiovasc. Surg. 66 (1973) 202–208.

[57] A. Tan, D. Holt, The effects of sterilization and storage treatments on the stress-strain behavior of aortic valve leaflets, Ann. Thorac. Surg. 22 (1976) 188–194, https://doi.org/10.1016/S0003-4975(10)63984-7.

[58] E. Rousseau, A. Sauren, M. Van Hout, A. Van Steenhoven, Elastic and viscoelastic material behaviour of fresh and glutaraldehyde-treated porcine aortic valve tissue, J. Biomech. 16 (1983) 339–348, https://doi.org/10.1016/0021-9290(83)90017-9.

[59] A. Sauren, M. Van Hout, A. Van Steenhoven, F. Veldpaus, J. Janssen, The mechanical properties of porcine aortic valve tissues, J. Biomech. 16 (1983) 327–337, https://doi.org/10.1016/0021-9290(83)90016-7.

[60] C.G. McGregor, A. Carpentier, N. Lila, J.S. Logan, G.W. Byrne, Cardiac xenotransplantation technology provides materials for improved bioprosthetic heart valves, J. Thorac. Cardiovasc. Surg. 141 (2011) 269–275, https://doi.org/10.1016/j.jtcvs.2010.08.064.

[61] N. Lila, C.G. McGregor, S. Carpentier, J. Rancic, G.W. Byrne, A. Carpentier, Gal knockout pig pericardium: new source of material for heart valve bioprostheses, J. Heart Lung Transplant. 29 (2010) 538–543, https://doi.org/10.1016/j.healun.2009.10.007.

[62] A. Salama, G. Evanno, J. Harb, J.P. Soulillou, Potential deleterious role of anti-Neu5Gc antibodies in xenotransplantation, Xenotransplantation 22 (2015) 85–94, https://doi.org/10.1111/xen.12142.

[63] R.A. Manji, W. Lee, D.K. Cooper, Xenograft bioprosthetic heart valves: past, present and future, Int. J. Surg. 23 (2015) 280–284, https://doi.org/10.1016/j.ijsu.2015.07.009.

[64] W. Lee, C. Long, J. Ramsoondar, D. Ayares, D.K. Cooper, R.A. Manji, H. Hara, Human antibody recognition of xenogeneic antigens (NeuGc and Gal) on porcine heart valves: could genetically modified pig heart valves reduce structural valve deterioration? Xenotransplantation 23 (2016) 370–380, https://doi.org/10.1111/xen.12254.

[65] W. Lee, H. Hara, D.K. Cooper, R.A. Manji, Expression of NeuGc on pig heart valves, Xenotransplantation 22 (2015) 153–154, https://doi.org/10.1111/xen.12162.

[66] B. Smood, H. Hara, D. Cleveland, D.K. Cooper, In search of the ideal valve: optimizing genetic modifications to prevent bioprosthetic degeneration, Ann. Thorac. Surg. 108 (2019) 624–635, https://doi.org/10.1016/j.athoracsur.2019.01.054.

[67] R.J. Crawford, Plastics Engineering, Butterworth-Heinemann, Oxford, 1998, p. 505.

[68] A. Balguid, M.P. Rubbens, A. Mol, R.A. Bank, A.J. Bogers, J.P. v Kats, B.A. d Mol, F.P. Baaijens, C.V. Bouten, The role of collagen cross-links in biomechanical behavior of human aortic heart valve leaflets—relevance for tissue engineering, Tissue Eng. 13 (2007) 1501–1511, https://doi.org/10.1089/ten.2006.0279.

[69] G.M. Bernacca, T.G. Mackay, R. Wilkinson, D.J. Wheatley, Polyurethane heart valves: fatigue failure, calcification, and polyurethane structure, J. Biomed. Mater. Res. 34 (1997) 371–379, https://doi.org/10.1002/(SICI)1097-4636(19970305)34:3<371::AID-JBM12>3.0.CO;2-J.

[70] G.M. Bernacca, B. O'Connor, D.F. Williams, D.J. Wheatley, Hydrodynamic function of polyurethane prosthetic heart valves: influences of Young's modulus and leaflet thickness, Biomaterials 23 (2002) 45–50, https://doi.org/10.1016/S0142-9612(01)00077-1.

[71] G.M. Bernacca, L. Raco, P.R. Belcher, D.J. Wheatley, I. Sim, J.S. Boyd, Polyurethane: material for the next generation of heart valve prostheses? Eur. J. Cardiothorac. Surg. 17 (2000) 440–448, https://doi.org/10.1016/S1010-7940(00)00381-X.

[72] K. Stokes, R. McVenes, J.M. Anderson, Polyurethane elastomer biostability, J. Biomater. Appl. 9 (1995) 321–354, https://doi.org/10.1177/088532829500900402.

[73] N.S. Braunwald, T. Cooper, A.G. Morrow, Complete replacement of the mitral valve. Successful clinical application of a flexible polyurethane prosthesis, J. Thorac. Cardiovasc. Surg. 40 (1960) 1–11.

[74] E.L. Gerring, B.J. Bellhouse, F.H. Bellhouse, W.S. Haworth, Long term animal trials of the oxford aortic/pulmonary valve prosthesis without anticoagulants, Am. Soc. Artif. Intern. Organs J. 20 (1974) 703–707.

[75] J.W. Boretos, W.S. Pierce, Segmented polyurethane: a new elastomer for biomedical applications, Science 158 (1967) 1481–1482, https://doi.org/10.1126/science.158.3807.1481 %J Science.

[76] C.B. Wisman, W.S. Pierce, J.H. Donachy, W.E. Pae, J.L. Myers, G.A. Prophet, A polyurethane trileaflet cardiac valve prosthesis: in vitro and in vivo studies, Am. Soc. Artif. Intern. Organs J. 28 (1982) 164–168.

[77] T.G. Mackay, D.J. Wheatley, G.M. Bernacca, A.C. Fisher, C.S. Hindle, New polyurethane heart valve prosthesis: design, manufacture and evaluation, Biomaterials 17 (1996) 1857–1863, https://doi.org/10.1016/0142-9612(95)00242-1.

[78] G.M. Bernacca, T.G. Mackay, R. Wilkinson, D.J. Wheatley, Calcification and fatigue failure in a polyurethane heart valve, Biomaterials 16 (1995) 279–285, https://doi.org/10.1016/0142-9612(95)93255-C.

[79] P. Boloori Zadeh, S.C. Corbett, H. Nayeb-Hashemi, In-vitro calcification study of polyurethane heart valves, Mater. Sci. Eng. C 35 (2014) 335–340, https://doi.org/10.1016/j.msec.2013.11.015.

[80] S.L. Hilbert, V.J. Ferrans, Y. Tomita, E.E. Eidbo, M. Jones, Evaluation of explanted polyurethane trileaflet cardiac valve prostheses, J. Thorac. Cardiovasc. Surg. 94 (1987) 419–429.

[81] R.R. Joshi, J.R. Frautschi, R.E. Phillips Jr., R.J. Levy, Phosphonated polyurethanes that resist calcification, J. Appl. Biomater. 5 (1994) 65–77, https://doi.org/10.1002/jab.770050109.

[82] S.H. Daebritz, B. Fausten, B. Hermanns, J. Schroeder, J. Groetzner, R. Autschbach, B.J. Messmer, J.S. Sachweh, Introduction of a flexible polymeric heart valve prosthesis with special design for aortic position, Eur. J. Cardiothorac. Surg. 25 (2004) 946–952, https://doi.org/10.1016/j.ejcts.2004.02.040.

[83] Y.W. Tang, R.S. Labow, J.P. Santerre, Enzyme-induced biodegradation of polycarbonate-polyurethanes: dependence on hard-segment chemistry, J. Biomed. Mater. Res. 57 (2001) 597–611, https://doi.org/10.1002/1097-4636(20011215)57:4<597::Aid-jbm1207>3.0.Co;2-t.

[84] H.J. Salacinski, M. Odlyha, G. Hamilton, A.M. Seifalian, Thermo-mechanical analysis of a compliant poly(carbonate-urea)urethane after exposure to hydrolytic, oxidative, peroxidative and biological solutions, Biomaterials 23 (2002) 2231–2240, https://doi.org/10.1016/S0142-9612(01)00356-8.

[85] S.H. Daebritz, J.S. Sachweh, B. Hermanns, B. Fausten, A. Franke, J. Groetzner, B. Klosterhalfen, B.J. Messmer, Introduction of a flexible polymeric heart valve prosthesis with special design for mitral position, Circulation 108 (2003), https://doi.org/10.1161/01.cir.0000087655.41288.dc. II-134–II-139.

[86] M.E. Leat, J. Fisher, The Influence of manufacturing methods on the function and performance of a synthetic leaflet heart valve, Proc. Inst. Mech. Eng., Part H 209 (1995) 65–69, https://doi.org/10.1243/pime_proc_1995_209_318_02.

[87] E. Bodnar, R.W.M. Frater, Replacement Cardiac Valves, Pergamon Press, 1991.

[88] A.G. Kidane, G. Burriesci, M. Edirisinghe, H. Ghanbari, P. Bonhoeffer, A.M. Seifalian, A novel nanocomposite polymer for development of synthetic heart valve leaflets, Acta Biomater. 5 (2009) 2409–2417, https://doi.org/10.1016/j.actbio.2009.02.025.

[89] R.Y. Kannan, H.J. Salacinski, J. De Groot, I. Clatworthy, L. Bozec, M. Horton, P.E. Butler, A.M. Seifalian, The antithrombogenic potential of a polyhedral oligomeric silsesquioxane (POSS) nanocomposite, Biomacromolecules 7 (2006) 215–223, https://doi.org/10.1021/bm050590z.

[90] P.J. Rae, E.N. Brown, The properties of poly(tetrafluoroethylene) (PTFE) in tension, Polymer 46 (2005) 8128–8140, https://doi.org/10.1016/j.polymer.2005.06.120.

[91] L.C.S. Nunes, F.W.R. Dias, H.S. da Costa Mattos, Mechanical behavior of polytetrafluoroethylene in tensile loading under different strain rates, Polym. Test. 30 (2011) 791–796, https://doi.org/10.1016/j.polymertesting.2011.07.004.

[92] N.S. Braunwald, A.G. Morrow, A late evaluation of flexible teflon prostheses utilized for total aortic valve replacement. Postoperative clinical, hemodynamic, and pathological assessments, J. Thorac. Cardiovasc. Surg. 49 (1965) 485–496.

[93] E. Imamura, M.P. Kaye, Function of expanded-polytetrafluoroethylene laminated trileaflet valves in animals, Mayo Clin. Proc. 52 (1978) 770–775.

[94] F. Nistal, V. García-Martínez, E. Arbe, D. Fernández, E. Artiñano, F. Mazorra, I. Gallo, In vivo experimental assessment of polytetrafluoroethylene trileaflet heart valve prosthesis, J. Thorac. Cardiovasc. Surg. 99 (1990) 1074–1081.

[95] J.A. Quintessenza, J.P. Jacobs, P.J. Chai, V.O. Morell, H. Lindberg, Polytetrafluoroethylene bicuspid pulmonary valve implantation: experience with 126 patients, World J. Pediatr. Congenit. Heart Surg. 1 (2010) 20–27, https://doi.org/10.1177/2150135110361509.

[96] J.A. Quintessenza, J.P. Jacobs, V.O. Morell, J.M. Giroud, R.J. Boucek, Initial experience with a bicuspid polytetrafluoroethylene pulmonary valve in 41 children and adults: a new option for right ventricular outflow tract reconstruction, Ann. Thorac. Surg. 79 (2005) 924–931, https://doi.org/10.1016/j.athoracsur.2004.05.045.

[97] K.H. Choi, S.C. Sung, H. Kim, H.D. Lee, G. Kim, H. Ko, Late results of right ventricular outflow tract reconstruction with a bicuspid expanded polytetrafluoroethylene valved conduit, J. Card. Surg. 33 (2018) 36–40, https://doi.org/10.1111/jocs.13507.

[98] L. Pinchuk, G.J. Wilson, J.J. Barry, R.T. Schoephoerster, J.-M. Parel, J.P. Kennedy, Medical applications of poly(styrene-block-isobutylene-block-styrene) ("SIBS"), Biomaterials 29 (2008) 448–460, https://doi.org/10.1016/j.biomaterials.2007.09.041.

[99] Qiang Wang, Anthony J. McGoron, Richard Bianco, Yasushi Kato, Pinchuk Leonard, R.T. Schoephoerster, In-vivo assessment of a novel polymer (SIBS) trileaflet heart valve, J. Heart Valve Dis. 19 (2010) 499–505.

[100] M. El Fray, P. Prowans, J.E. Puskas, V. Altstädt, Biocompatibility and fatigue properties of Polystyrene−Polyisobutylene−Polystyrene, an emerging thermoplastic elastomeric biomaterial, Biomacromolecules 7 (2006) 844–850, https://doi.org/10.1021/bm050971c.

[101] T.E. Claiborne, J. Sheriff, M. Kuetting, U. Steinseifer, M.J. Slepian, D. Bluestein, In vitro evaluation of a novel hemodynamically optimized trileaflet polymeric prosthetic heart valve, J. Biomech. Eng. 135 (2013), 021021, https://doi.org/10.1115/1.4023235.

[102] F. Li, Y. Su, G. Pi, P.X. Ma, B. Lei, Biodegradable, Biomimetic elastomeric, photoluminescent, and broad-spectrum antibacterial polycitrate-polypeptide-based membrane toward multifunctional biomedical implants, ACS Biomater. Sci. Eng. 4 (2018) 3027–3035, https://doi.org/10.1021/acsbiomaterials.8b00660.

[103] R.N. Reusch, A.W. Sparrow, J. Gardiner, Transport of poly-β-hydroxybutyrate in human plasma, Biochim. Biophys. Acta Lipids Lipid Metab. 1123 (1992) 33–40, https://doi.org/10.1016/0005-2760(92)90168-U.

[104] E.E. Kaufman, N. Relkin, T. Nelson, Regulation and properties of an NADP+ oxidoreductase which functions as a γ-Hydroxybutyrate dehydrogenase, J. Neurochem. 40 (1983) 1639–1646, https://doi.org/10.1111/j.1471-4159.1983.tb08137.x.

[105] T. Shinoka, C.K. Breuer, R.E. Tanel, G. Zund, T. Miura, P.X. Ma, R. Langer, J.P. Vacanti, J.E. Mayer, Tissue engineering heart valves: valve leaflet replacement study in a lamb model, Ann. Thorac. Surg. 60 (1995) S513–S516, https://doi.org/10.1016/0003-4975(95)00733-4.

[106] U.A. Stock, M. Nagashima, P.N. Khalil, G.D. Nollert, T. Herden, J.S. Sperling, A. Moran, J. Lien, D.P. Martin, F.J. Schoen, J.P. Vacanti, J.E. Mayer, Tissue-engineered valved conduits in the pulmonary circulation, J. Thorac. Cardiovasc. Surg. 119 (2000) 732–740, https://doi.org/10.1016/S0022-5223(00)70008-0.

[107] D.P. Martin, S.F. Williams, Medical applications of poly-4-hydroxybutyrate: a strong flexible absorbable biomaterial, Biochem. Eng. J. 16 (2003) 97–105, https://doi.org/10.1016/S1369-703X(03)00040-8.

[108] P. Hoerstrup Simon, R. Sodian, S. Daebritz, J. Wang, A. Bacha Emile, P. Martin David, M. Moran Adrian, J. Guleserian Kristine, S. Sperling Jason, S. Kaushal, P. Vacanti Joseph, J. Schoen Frederick, E. Mayer John, Functional living trileaflet heart valves grown in vitro, Circulation 102 (2000) Iii44–49, https://doi.org/10.1161/circ.102.suppl_3.III-44.

[109] L. Hench, J. Jones, Biomaterials, Artificial Organs and Tissue Engineering, first ed., Elsevier, 2005.

[110] T. Shinoka, D. Shum-Tim, P.X. Ma, R.E. Tanel, N. Isogai, R. Langer, J.P. Vacanti, J.E. Mayer, Creation of viable pulmonary artery autografts through tissue engineering, J. Thorac. Cardiovasc. Surg. 115 (1998) 536–546, https://doi.org/10.1016/S0022-5223(98)70315-0.

[111] D. Shum-Tim, U. Stock, J. Hrkach, T. Shinoka, J. Lien, M.A. Moses, A. Stamp, G. Taylor, A.M. Moran, W. Landis, R. Langer, J.P. Vacanti, J.E. Mayer, Tissue engineering of autologous aorta using a new biodegradable polymer, Ann. Thorac. Surg. 68 (1999) 2298–2304, https://doi.org/10.1016/S0003-4975(99)01055-3.

[112] K. Schenke-Layland, T.U. Cohnert, U.A. Stock, F. Opitz, B. Starcher, K.J. Halbhuber, D.P. Martin, Tissue engineering of aortic tissue: dire consequence of suboptimal elastic fiber synthesis in vivo, Cardiovasc. Res. 63 (2004) 719–730, https://doi.org/10.1016/j.cardiores.2004.05.002.

[113] S. Naficy, H.R. Brown, J.M. Razal, G.M. Spinks, P.G. Whitten, Progress toward robust polymer hydrogels, Aust. J. Chem. 64 (2011) 1007–1025, https://doi.org/10.1071/CH11156.

[114] F. Oveissi, S. Naficy, T.Y.L. Le, D.F. Fletcher, F. Dehghani, Tough hydrophilic polyurethane-based hydrogels with mechanical properties similar to human soft tissues, J. Mater. Chem. B. 7 (2019) 3512–3519, https://doi.org/10.1039/C9TB00080A.

[115] R. Bai, J. Yang, Z. Suo, Fatigue of hydrogels, Eur. J. Mech. A Solid. 74 (2019) 337–370, https://doi.org/10.1016/j.euromechsol.2018.12.001.

[116] N.T. Lam, H. Lam, N.M. Sturdivant, K. Balachandran, Fabrication of a matrigel–collagen semi-interpenetrating scaffold for use in dynamic valve interstitial cell culture, Biomed. Mater. 12 (2017), 045013, https://doi.org/10.1088/1748-605x/aa71be.

[117] S. Rhee, J.L. Puetzer, B.N. Mason, C.A. Reinhart-King, L.J. Bonassar, 3D bioprinting of spatially heterogeneous collagen constructs for cartilage tissue engineering, ACS Biomater. Sci. Eng. 2 (2016) 1800–1805, https://doi.org/10.1021/acsbiomaterials.6b00288.

[118] X. Zhang, B. Xu, D.S. Puperi, Y. Wu, J.L. West, K.J. Grande-Allen, Application of hydrogels in heart valve tissue engineering, J. Long Term Eff. Med. Implant. 25 (2015) 105–134, https://doi.org/10.1615/JLongTermEffMedImplants.2015011817.

[119] P.S. Gungor-Ozkerim, I. Inci, Y.S. Zhang, A. Khademhosseini, M.R. Dokmeci, Bioinks for 3D bioprinting: an overview, Biomater. Sci. 6 (2018) 915–946, https://doi.org/10.1039/C7BM00765E.

[120] X. Liu, H. Yuk, S. Lin, G.A. Parada, T.-C. Tang, E. Tham, C. de la Fuente-Nunez, T.K. Lu, X. Zhao, 3D Printing of living responsive materials and devices, Adv. Mater. 30 (2018) 1704821, https://doi.org/10.1002/adma.201704821.

[121] C. Xu, W. Lee, G. Dai, Y. Hong, Highly elastic biodegradable single-network hydrogel for cell printing, ACS Appl. Mater. Interfaces 10 (2018) 9969–9979, https://doi.org/10.1021/acsami.8b01294.

[122] A.K. Capulli, M.Y. Emmert, F.S. Pasqualini, D. Kehl, E. Caliskan, J.U. Lind, S.P. Sheehy, S.J. Park, S. Ahn, B. Weber, J.A. Goss, S.P. Hoerstrup, K.K. Parker, JetValve: rapid manufacturing of biohybrid scaffolds for biomimetic heart valve replacement, Biomaterials 133 (2017) 229–241, https://doi.org/10.1016/j.biomaterials.2017.04.033.

[123] W. Miriam, G.d.T. Israel, M. Ricardo, F. Julia, O. Caroline, A. Matilde, R.C. C J, J. Stefan, M. Petra, Multiple-step injection molding for fibrin-based tissue-engineered heart valves, Tissue Eng. Part C 21 (2015) 832–840, https://doi.org/10.1089/ten.tec.2014.0396.

[124] R. Moreira, C. Neusser, M. Kruse, S. Mulderrig, F. Wolf, J. Spillner, T. Schmitz-Rode, S. Jockenhoevel, P. Mela, Tissue-engineered fibrin-based heart valve with bio-inspired textile reinforcement, Adv. Healthc. Mater. 5 (2016) 2113–2121, https://doi.org/10.1002/adhm.201600300.

[125] B. Duan, L.A. Hockaday, K.H. Kang, J.T. Butcher, 3D Bioprinting of heterogeneous aortic valve conduits with alginate/gelatin hydrogels, J. Biomed. Mater. Res. A 101A (2013) 1255–1264, https://doi.org/10.1002/jbm.a.34420.

[126] K. Haraguchi, T. Takehisa, Nanocomposite hydrogels: a unique organic–inorganic network structure with extraordinary mechanical, optical, and swelling/de-swelling properties, Adv. Mater. 14 (2002) 1120–1124, https://doi.org/10.1002/1521-4095(20020816)14:16<1120::AID-ADMA1120>3.0.CO;2-9.

[127] J.P. Gong, Y. Katsuyama, T. Kurokawa, Y. Osada, Double-network hydrogels with extremely high mechanical strength, Adv. Mater. 15 (2003) 1155–1158, https://doi.org/10.1002/adma.200304907.

[128] J.-X. Chen, J. Yuan, Y.-L. Wu, P. Wang, P. Zhao, G.-Z. Lv, J.-H. Chen, Fabrication of tough poly(ethylene glycol)/collagen double network hydrogels for tissue engineering, J. Biomed. Mater. Res. A. 106 (2018) 192–200, https://doi.org/10.1002/jbm.a.36222.

[129] X. Zhao, Multi-scale multi-mechanism design of tough hydrogels: building dissipation into stretchy networks, Soft Matter 10 (2014) 672–687, https://doi.org/10.1039/C3SM52272E.

[130] M. Guo, L.M. Pitet, H.M. Wyss, M. Vos, P.Y.W. Dankers, E.W. Meijer, Tough stimuli-responsive supramolecular hydrogels with hydrogen-bonding network Junctions, J. Am. Chem. Soc. 136 (2014) 6969–6977, https://doi.org/10.1021/ja500205v.

[131] X.N. Zhang, Y.J. Wang, S. Sun, L. Hou, P. Wu, Z.L. Wu, Q. Zheng, A Tough and stiff hydrogel with tunable water content and mechanical properties based on the synergistic effect of hydrogen bonding and hydrophobic interaction, Macromolecules 51 (2018) 8136–8146, https://doi.org/10.1021/acs.macromol.8b01496.

[132] T.L. Sun, T. Kurokawa, S. Kuroda, A.B. Ihsan, T. Akasaki, K. Sato, M.A. Haque, T. Nakajima, J.P. Gong, Physical hydrogels composed of polyampholytes demonstrate high toughness and viscoelasticity, Nat. Mater. 12 (2013) 932, https://doi.org/10.1038/nmat3713.

[133] J.L. Mann, A.C. Yu, G. Agmon, E.A. Appel, Supramolecular polymeric biomaterials, Biomater. Sci. 6 (2018) 10–37, https://doi.org/10.1039/C7BM00780A.

[134] C. Shao, M. Wang, L. Meng, H. Chang, B. Wang, F. Xu, J. Yang, P. Wan, Mussel-inspired cellulose nanocomposite tough hydrogels with synergistic self-healing, adhesive, and strain-sensitive properties, Chem. Mater. 30 (2018) 3110–3121, https://doi.org/10.1021/acs.chemmater.8b01172.

[135] L. Wu, Z. Zhuang, S. Li, X. Ma, W. Diao, X. Bu, Y. Fang, Ultrastretchable, super tough, and rapidly recoverable nanocomposite double-network hydrogels by dual physically hydrogen bond and vinyl-functionalized silica nanoparticles macro-crosslinking, Macromol. Mater. Eng. 304 (2019) 1800737, https://doi.org/10.1002/mame.201800737.

[136] F. Oveissi, S. Naficy, T.Y.L. Le, D.F. Fletcher, F. Dehghani, Tough and processable hydrogels based on lignin and hydrophilic polyurethane, ACS Appl. Bio Mater. 1 (2018) 2073–2081, https://doi.org/10.1021/acsabm.8b00546.

[137] J.-Y. Sun, X. Zhao, W.R.K. Illeperuma, O. Chaudhuri, K.H. Oh, D.J. Mooney, J.J. Vlassak, Z. Suo, Highly stretchable and tough hydrogels, ON Nat. 489 (2012) 133. https://10.1038/nature11409.

[138] J. Li, W.R.K. Illeperuma, Z. Suo, J.J. Vlassak, Hybrid hydrogels with extremely high stiffness and toughness, ACS Macro Lett. 3 (2014) 520–523, https://doi.org/10.1021/mz5002355.

[139] M.A. Gonzalez, J.R. Simon, A. Ghoorchian, Z. Scholl, S. Lin, M. Rubinstein, P. Marszalek, A. Chilkoti, G.P. López, X. Zhao, Strong, tough, stretchable, and self-adhesive hydrogels from intrinsically unstructured proteins, Adv. Mater. 29 (2017) 1604743, https://doi.org/10.1002/adma.201604743.

[140] C. Loebel, A. Ayoub, J.H. Galarraga, O. Kossover, H. Simaan-Yameen, D. Seliktar, J.A. Burdick, Tailoring supramolecular guest–host hydrogel viscoelasticity with covalent fibrinogen double networks, J. Mater. Chem. B. 7 (2019) 1753–1760, https://doi.org/10.1039/C8TB02593B.

[141] F. Oveissi, S. Naficy, T.Y.L. Le, D.F. Fletcher, F. Dehghani, Polypeptide-affined interpenetrating hydrogels with tunable physical and mechanical properties, Biomater. Sci. 7 (2019) 926–937, https://doi.org/10.1039/C8BM01182F.

[142] R. Sodian, S.P. Hoerstrup, J.S. Sperling, S. Daebritz, D.P. Martin, A.M. Moran, B.S. Kim, F.J. Schoen, J.P. Vacanti, J.E. Mayer Jr., Early in vivo experience with tissue-engineered trileaflet heart valves, Circulation 102 (2000) Iii22–29, https://doi.org/10.1161/01.cir.102.suppl_3.iii-22.

[143] U.A. Stock, M. Nagashima, P.N. Khalil, G.D. Nollert, T. Herdena, J.S. Sperling, A. Moran, J. Lien, D.P. Martin, F.J. Schoen, Tissue-engineered valved conduits in the pulmonary circulation, J. Thorac. Cardiovasc. Surg. 119 (2000) 732–740, https://doi.org/10.1016/S0022-5223(00)70008-0.

[144] P.W. Serruys, Y. Miyazaki, A. Katsikis, M. Abdelghani, M.B. Leon, R. Virmani, T. Carrel, M. Cox, Y. Onuma, O.I. Soliman, Restorative valve therapy by endogenous tissue restoration: tomorrow's world? Reflection on the EuroPCR 2017 session on endogenous tissue restoration, Eur. Intervent. 13 (2017) AA68–77, https://doi.org/10.4244/EIJ-D-17-00509.

[145] J. Kluin, H. Talacua, A.I. Smits, M.Y. Emmert, M.C. Brugmans, E.S. Fioretta, P.E. Dijkman, S.H. Söntjens, R. Duijvelshoff, S. Dekker, In situ heart valve tissue engineering using a bioresorbable elastomeric implant–From material design to 12 months follow-up in sheep, Biomaterials 125 (2017) 101–117, https://doi.org/10.1016/j.biomaterials.2017.02.007.

[146] D. Schmidt, P.E. Dijkman, A. Driessen-Mol, R. Stenger, C. Mariani, A. Puolakka, M. Rissanen, T. Deichmann, B. Odermatt, B. Weber, Minimally-invasive implantation of living tissue engineered heart valves: a comprehensive approach from autologous vascular cells to stem cells, J. Am. Coll. Cardiol. 56 (2010) 510–520, https://doi.org/10.1016/j.jacc.2010.04.024.

[147] M. Weber, I. Gonzalez de Torre, R. Moreira, J. Frese, C. Oedekoven, M. Alonso, C.J. Rodriguez Cabello, S. Jockenhoevel, P. Mela, Multiple-step injection molding for fibrin-based tissue-engineered heart valves, Tissue Eng. Part C 21 (2015) 832–840, https://doi.org/10.1089/ten.TEC.2014.0396.

[148] T. Ondarçuhu, C. Joachim, Drawing a single nanofibre over hundreds of microns, Europhys. Lett. 42 (1998) 215–220, https://doi.org/10.1209/epl/i1998-00233-9.

[149] K. Strnadová, L. Stanislav, I. Krabicová, F. Sabol, J. Lukášek, M. Řezanka, D. Lukáš, V. Jenčová, Drawn aligned polymer microfibres for tissue engineering, J. Ind. Text. (2019) 1–15, https://doi.org/10.1177/1528083718825318.

[150] S. Agarwal, J.H. Wendorff, A. Greiner, Progress in the field of electrospinning for tissue engineering applications, Adv. Mater. 21 (2009) 3343–3351, https://doi.org/10.1002/adma.200803092.

[151] J.A. Matthews, G.E. Wnek, D.G. Simpson, G.L. Bowlin, Electrospinning of collagen nanofibers, Biomacromolecules 3 (2002) 232–238, https://doi.org/10.1021/bm015533u.

[152] X. Geng, O.-H. Kwon, J. Jang, Electrospinning of chitosan dissolved in concentrated acetic acid solution, Biomaterials 26 (2005) 5427–5432, https://doi.org/10.1016/j.biomaterials.2005.01.066.

[153] M.Z. Elsabee, H.F. Naguib, R.E. Morsi, Chitosan based nanofibers, review, Mater. Sci. Eng. C 32 (2012) 1711–1726, https://doi.org/10.1016/j.msec.2012.05.009.

[154] Z.-M. Huang, Y.Z. Zhang, S. Ramakrishna, C.T. Lim, Electrospinning and mechanical characterization of gelatin nanofibers, Polymer 45 (2004) 5361–5368, https://doi.org/10.1016/j.polymer.2004.04.005.

[155] G.E. Wnek, M.E. Carr, D.G. Simpson, G.L. Bowlin, Electrospinning of nanofiber fibrinogen structures, Nano Lett. 3 (2003) 213–216, https://doi.org/10.1021/nl025866c.

[156] B.-M. Min, S.W. Lee, J.N. Lim, Y. You, T.S. Lee, P.H. Kang, W.H. Park, Chitin and chitosan nanofibers: electrospinning of chitin and deacetylation of chitin nanofibers, Polymer 45 (2004) 7137–7142, https://doi.org/10.1016/j.polymer.2004.08.048.

[157] Y. Ji, K. Ghosh, X.Z. Shu, B. Li, J.C. Sokolov, G.D. Prestwich, R.A.F. Clark, M.H. Rafailovich, Electrospun three-dimensional hyaluronic acid nanofibrous scaffolds, Biomaterials 27 (2006) 3782–3792, https://doi.org/10.1016/j.biomaterials.2006.02.037.

[158] B.-M. Min, G. Lee, S.H. Kim, Y.S. Nam, T.S. Lee, W.H. Park, Electrospinning of silk fibroin nanofibers and its effect on the adhesion and spreading of normal human keratinocytes and fibroblasts in vitro, Biomaterials 25 (2004) 1289–1297, https://doi.org/10.1016/j.biomaterials.2003.08.045.

[159] N.J. Amoroso, A. D'Amore, Y. Hong, W.R. Wagner, M.S. Sacks, Elastomeric electrospun polyurethane scaffolds: the interrelationship between fabrication Conditions, fiber topology, and mechanical properties, J. Mech. Behav. Biomed. Mater. 23 (2011) 106–111, https://doi.org/10.1002/adma.201003210.

[160] M. Kitsara, O. Agbulut, D. Kontziampasis, Y. Chen, P. Menasché, Fibers for hearts: a critical review on electrospinning for cardiac tissue engineering, Acta Biomater. 48 (2017) 20–40, https://doi.org/10.1016/j.actbio.2016.11.014.

[161] G. Macchiarelli, O. Ohtani, S.A. Nottola, T. Stallone, A. Camboni, I.M. Prado, P.M. Motta, A micro-anatomical model of the distribution of myocardial endomysial collagen, Histol. Histopathol. 17 (2002) 699–706.

[162] P.J. Hanley, A.A. Young, I.J. LeGrice, S.G. Edgar, D.S. Loiselle, 3-Dimensional configuration of perimysial collagen fibres in rat cardiac muscle at resting and extended sarcomere lengths, J. Physiol. 517 (1999) 831–837, https://doi.org/10.1111/j.1469-7793.1999.0831s.x.

[163] J.W. Holmes, T.K. Borg, J.W. Covell, Structure and mechanics of healing myocardial infarcts, Annu. Rev. Biomed. Eng. 7 (2005) 223–253, https://doi.org/10.1146/annurev.bioeng.7.060804.100453.

[164] N.J. Amoroso, A. D'Amore, Y. Hong, C.P. Rivera, M.S. Sacks, W.R. Wagner, Microstructural manipulation of electrospun scaffolds for specific bending stiffness for heart valve tissue engineering, Acta Biomater. 8 (2012) 4268–4277, https://doi.org/10.1016/j.actbio.2012.08.002.

[165] S. Sant, C.M. Hwang, S.-H. Lee, A. Khademhosseini, Hybrid PGS–PCL microfibrous scaffolds with improved mechanical and biological properties, J. Tissue Eng. Regenerat. Med. 5 (2011) 283–291, https://doi.org/10.1002/term.313.

[166] D.-H. Paik, K.-Y. Jeong, S.-K. Moon, M.-J. Oh, T.-K. Ryu, S.-E. Kim, J.-H. Kim, J.-H. Park, S.-W. Choi, A facile method for preparation of polycaprolactone/tricalcium phosphate fibrous matrix with a gradient mineral content, Colloids Surf. A 429 (2013) 134–141, https://doi.org/10.1016/j.colsurfa.2013.03.063.

[167] C.P. Grey, S.T. Newton, G.L. Bowlin, T.W. Haas, D.G. Simpson, Gradient fiber electrospinning of layered scaffolds using controlled transitions in fiber diameter, Biomaterials 34 (2013) 4993–5006, https://doi.org/10.1016/j.biomaterials.2013.03.033.

[168] M.R. Ladd, S.J. Lee, J.D. Stitzel, A. Atala, J.J. Yoo, Co-electrospun dual scaffolding system with potential for muscle–tendon junction tissue engineering, Biomaterials 32 (2011) 1549–1559, https://doi.org/10.1016/j.biomaterials.2010.10.038.
[169] X. Zhang, X. Gao, L. Jiang, J. Qin, Flexible Generation of gradient electrospinning nanofibers using a microfluidic assisted approach, Langmuir 28 (2012) 10026–10032, https://doi.org/10.1021/la300821r.
[170] A.P. Kishan, A.B. Robbins, S.F. Mohiuddin, M. Jiang, M.R. Moreno, E.M. Cosgriff-Hernandez, Fabrication of macromolecular gradients in aligned fiber scaffolds using a combination of in-line blending and air-gap electrospinning, Acta Biomater. 56 (2017) 118–128, https://doi.org/10.1016/j.actbio.2016.12.041.
[171] H.G. Sundararaghavan, J.A. Burdick, Gradients with depth in electrospun fibrous scaffolds for directed cell behavior, Biomacromolecules 12 (2011) 2344–2350, https://doi.org/10.1021/bm200415g.
[172] S. Hinderer, J. Seifert, M. Votteler, N. Shen, J. Rheinlaender, T.E. Schäffer, K. Schenke-Layland, Engineering of a bio-functionalized hybrid off-the-shelf heart valve, Biomaterials 35 (2014) 2130–2139, https://doi.org/10.1016/j.biomaterials.2013.10.080.
[173] A. D'Amore, S.K. Luketich, G.M. Raffa, S. Olia, G. Menallo, A. Mazzola, F. D'Accardi, T. Grunberg, X. Gu, M. Pilato, M.V. Kameneva, V. Badhwar, W.R. Wagner, Heart valve scaffold fabrication: bioinspired control of macro-scale morphology, mechanics and micro-structure, Biomaterials 150 (2018) 25–37, https://doi.org/10.1016/j.biomaterials.2017.10.011.
[174] D.S. Puperi, A. Kishan, Z.E. Punske, Y. Wu, E. Cosgriff-Hernandez, J.L. West, K.J. Grande-Allen, Electrospun polyurethane and hydrogel composite scaffolds as biomechanical mimics for aortic valve tissue engineering, ACS Biomater. Sci. Eng. 2 (2016) 1546–1558, https://doi.org/10.1021/acsbiomaterials.6b00309.
[175] J.H. Chung, S. Naficy, Z. Yue, R. Kapsa, A. Quigley, S.E. Moulton, G.G. Wallace, Bio-ink properties and printability for extrusion printing living cells, Biomater. Sci. 1 (2013) 763–773, https://doi.org/10.1039/C3BM00012E.
[176] S.V. Murphy, A. Atala, 3D bioprinting of tissues and organs, Nat. Biotechnol. 32 (2014) 773, https://doi.org/10.1038/nbt.2958.
[177] J. Malda, J. Visser, F.P. Melchels, T. Jüngst, W.E. Hennink, W.J.A. Dhert, J. Groll, D.W. Hutmacher, 25th anniversary article: engineering hydrogels for biofabrication, Adv. Mater. 25 (2013) 5011–5028, https://doi.org/10.1002/adma.201302042.
[178] T. Jiang, J.G. Munguia-Lopez, S. Flores-Torres, J. Kort-Mascort, J.M. Kinsella, Extrusion bioprinting of soft materials: an emerging technique for biological model fabrication, Appl. Phys. Rev. 6 (2019), 011310, https://doi.org/10.1063/1.5059393.
[179] G. Gao, B.S. Kim, J. Jang, D.-W. Cho, Recent strategies in extrusion-based three-dimensional cell printing toward organ biofabrication, ACS Biomater. Sci. Eng. 5 (2019) 1150–1169, https://doi.org/10.1021/acsbiomaterials.8b00691.
[180] I.T. Ozbolat, M. Hospodiuk, Current advances and future perspectives in extrusion-based bioprinting, Biomaterials 76 (2016) 321–343, https://doi.org/10.1016/j.biomaterials.2015.10.076.
[181] J. Jang, H.-G. Yi, D.-W. Cho, 3D printed tissue models: present and future, ACS Biomater. Sci. Eng. 2 (2016) 1722–1731, https://doi.org/10.1021/acsbiomaterials.6b00129.
[182] C.S. Ong, P. Yesantharao, C.Y. Huang, G. Mattson, J. Boktor, T. Fukunishi, H. Zhang, N. Hibino, 3D bioprinting using stem cells, Pediatr. Res. 83 (2017) 223, https://doi.org/10.1038/pr.2017.252.
[183] J.M. Lee, W.L. Ng, W.Y. Yeong, Resolution and shape in bioprinting: strategizing towards complex tissue and organ printing, Appl. Phys. Rev. 6 (2019), 011307, https://doi.org/10.1063/1.5053909.
[184] P. Jiang, C. Yan, Y. Guo, X. Zhang, M. Cai, X. Jia, X. Wang, F. Zhou, Direct ink writing with high-strength and swelling-resistant biocompatible physically crosslinked hydrogels, Biomater. Sci. 7 (2019) 1805–1814, https://doi.org/10.1039/C9BM00081J.
[185] J. Jia, D.J. Richards, S. Pollard, Y. Tan, J. Rodriguez, R.P. Visconti, T.C. Trusk, M.J. Yost, H. Yao, R.R. Markwald, Y. Mei, Engineering alginate as bioink for bioprinting, Acta Biomater. 10 (2014) 4323–4331, https://doi.org/10.1016/j.actbio.2014.06.034.
[186] T. Billiet, E. Gevaert, T. De Schryver, M. Cornelissen, P. Dubruel, The 3D printing of gelatin methacrylamide cell-laden tissue-engineered constructs with high cell viability, Biomaterials 35 (2014) 49–62, https://doi.org/10.1016/j.biomaterials.2013.09.078.
[187] L.E. Bertassoni, J.C. Cardoso, V. Manoharan, A.L. Cristino, N.S. Bhise, W.A. Araujo, P. Zorlutuna, N.E. Vrana, A.M. Ghaemmaghami, M.R. Dokmeci, A. Khademhosseini, Direct-write bioprinting of cell-laden methacrylated gelatin hydrogels, Biofabrication 6 (2014), 024105, https://doi.org/10.1088/1758-5082/6/2/024105.
[188] N.E. Fedorovich, J.R.D. Wijn, A.J. Verbout, J. Alblas, W.J.A. Dhert, Three-dimensional fiber deposition of cell-laden, viable, patterned constructs for bone tissue printing, Tissue Eng. A 14 (2008) 127–133, https://doi.org/10.1089/ten.a.2007.0158.
[189] M. Yeo, J.-S. Lee, W. Chun, G.H. Kim, An innovative collagen-based cell-printing method for obtaining human adipose stem cell-laden structures consisting of core–sheath structures for tissue engineering, Biomacromolecules 17 (2016) 1365–1375, https://doi.org/10.1021/acs.biomac.5b01764.
[190] H.-W. Kang, S.J. Lee, I.K. Ko, C. Kengla, J.J. Yoo, A. Atala, A 3D bioprinting system to produce human-scale tissue constructs with structural integrity, Nat. Biotechnol. 34 (2016) 312, https://doi.org/10.1038/nbt.3413.
[191] S. Das, F. Pati, Y.-J. Choi, G. Rijal, J.-H. Shim, S.W. Kim, A.R. Ray, D.-W. Cho, S. Ghosh, Bioprintable, cell-laden silk fibroin–gelatin hydrogel supporting multilineage differentiation of stem cells for fabrication of three-dimensional tissue constructs, Acta Biomater. 11 (2015) 233–246, https://doi.org/10.1016/j.actbio.2014.09.023.
[192] K. Schacht, T. Jüngst, M. Schweinlin, A. Ewald, J. Groll, T. Scheibel, Biofabrication of cell-loaded 3D spider silk constructs, Angew. Chem. Int. Ed. 54 (2015) 2816–2820, https://doi.org/10.1002/anie.201409846.
[193] L. Ouyang, C.B. Highley, W. Sun, J.A. Burdick, A generalizable strategy for the 3D bioprinting of hydrogels from nonviscous photo-crosslinkable Inks, Adv. Mater. 29 (2017) 1604983, https://doi.org/10.1002/adma.201604983.
[194] C.B. Highley, C.B. Rodell, J.A. Burdick, Direct 3D printing of shear-thinning hydrogels into self-healing hydrogels, Adv. Mater. 27 (2015) 5075–5079, https://doi.org/10.1002/adma.201501234.
[195] P. Datta, B. Ayan, I.T. Ozbolat, Bioprinting for vascular and vascularized tissue biofabrication, Acta Biomater. 51 (2017) 1–20, https://doi.org/10.1016/j.actbio.2017.01.035.
[196] D.B. Kolesky, R.L. Truby, A.S. Gladman, T.A. Busbee, K.A. Homan, J.A. Lewis, 3D bioprinting of vascularized, heterogeneous cell-laden tissue constructs, Adv. Mater. 26 (2014) 3124–3130, https://doi.org/10.1002/adma.201305506.
[197] K. Nair, M. Gandhi, S. Khalil, K.C. Yan, M. Marcolongo, K. Barbee, W. Sun, Characterization of cell viability during bioprinting processes, Biotechnol. J. 4 (2009) 1168–1177, https://doi.org/10.1002/biot.200900004.
[198] W. Liu, Y.S. Zhang, M.A. Heinrich, F. De Ferrari, H.L. Jang, S.M. Bakht, M.M. Alvarez, J. Yang, Y.-C. Li, G. Trujillo-de Santiago, A.K. Miri, K. Zhu, P. Khoshakhlagh, G. Prakash, H. Cheng, X. Guan, Z. Zhong, J. Ju, G.H. Zhu, X. Jin, S.R. Shin, M.R. Dokmeci, A. Khademhosseini, Rapid continuous multimaterial extrusion bioprinting, Adv. Mater. 29 (2017) 1604630, https://doi.org/10.1002/adma.201604630.
[199] L.G. Bracaglia, B.T. Smith, E. Watson, N. Arumugasaamy, A.G. Mikos, J.P. Fisher, 3D printing for the design and fabrication of polymer-based gradient scaffolds, Acta Biomater. 56 (2017) 3–13, https://doi.org/10.1016/j.actbio.2017.03.030.
[200] H. Liu, Y. Sun, C.A. Simmons, Determination of local and global elastic moduli of valve interstitial cells cultured on soft substrates, J. Biomech. 46 (2013) 1967–1971, https://doi.org/10.1016/j.jbiomech.2013.05.001.
[201] L.A. Hockaday, K.H. Kang, N.W. Colangelo, P.Y.C. Cheung, B. Duan, E. Malone, J. Wu, L.N. Girardi, L.J. Bonassar, H. Lipson, C.C. Chu, J.T. Butcher, Rapid 3D printing of anatomically accurate and mechanically heterogeneous aortic valve hydrogel scaffolds, Biofabrication 4 (2012), 035005, https://doi.org/10.1088/1758-5082/4/3/035005.
[202] H.L. Ann, D. Bin, K.K. Heeyong, B.J. Talbot, 3D-printed hydrogel technologies for tissue-engineered heart valves, 3D Print. Addit. Manuf. 1 (2014) 122–136, https://doi.org/10.1089/3dp.2014.0018.
[203] B. Duan, E. Kapetanovic, L.A. Hockaday, J.T. Butcher, Three-dimensional printed trileaflet valve conduits using biological hydrogels and human valve interstitial cells, Acta Biomater. 10 (2014) 1836–1846, https://doi.org/10.1016/j.actbio.2013.12.005.
[204] L.H. Kang, P.A. Armstrong, L.J. Lee, B. Duan, K.H. Kang, J.T. Butcher, Optimizing photo-encapsulation viability of heart valve cell types in 3D printable composite hydrogels, Ann. Biomed. Eng. 45 (2017) 360–377, https://doi.org/10.1007/s10439-016-1619-1.
[205] J. Jang, H.-J. Park, S.-W. Kim, H. Kim, J.Y. Park, S.J. Na, H.J. Kim, M.N. Park, S.H. Choi, S.H. Park, S.W. Kim, S.-M. Kwon, P.-J. Kim, D.-W. Cho, 3D printed complex tissue construct using stem cell-laden decellularized extracellular matrix bioinks for cardiac repair, Biomaterials 112 (2017) 264–274, https://doi.org/10.1016/j.biomaterials.2016.10.026.
[206] L.T. Saldin, M.C. Cramer, S.S. Velankar, L.J. White, S.F. Badylak, Extracellular matrix hydrogels from decellularized tissues: structure and function, Acta Biomater. 49 (2017) 1–15, https://doi.org/10.1016/j.actbio.2016.11.068.
[207] M. Hospodiuk, M. Dey, D. Sosnoski, I.T. Ozbolat, The bioink: a comprehensive review on bioprintable materials, Biotechnol. Adv. 35 (2017) 217–239, https://doi.org/10.1016/j.biotechadv.2016.12.006.
[208] E. Garreta, R. Oria, C. Tarantino, M. Pla-Roca, P. Prado, F. Fernández-Avilés, J.M. Campistol, J. Samitier, N. Montserrat, Tissue engineering by decellularization and 3D bioprinting, Mater. Today 20 (2017) 166–178, https://doi.org/10.1016/j.mattod.2016.12.005.
[209] J. Jang, T.G. Kim, B.S. Kim, S.-W. Kim, S.-M. Kwon, D.-W. Cho, Tailoring mechanical properties of decellularized extracellular matrix bioink by vitamin B2-induced photo-crosslinking, Acta Biomater. 33 (2016) 88–95, https://doi.org/10.1016/j.actbio.2016.01.013.
[210] C. Kucukgul, S.B. Ozler, I. Inci, E. Karakas, S. Irmak, D. Gozuacik, A. Taralp, B. Koc, 3D bioprinting of biomimetic aortic vascular constructs with self-supporting cells, Biotechnol. Bioeng. 112 (2015) 811–821, https://doi.org/10.1002/bit.25493.
[211] J.P. Gong, Why are double network hydrogels so tough? Soft Matter 6 (2010) 2583–2590, https://doi.org/10.1039/B924290B.
[212] P.J. Joyce, J.A. Joyce, Evaluation of the fracture toughness properties of polytetrafluoroethylene, Int. J. Fract. 127 (2004) 361–385, https://doi.org/10.1023/B:FRAC.0000037674.46965.fb.
[213] N. Masoumi, A. Jean, J.T. Zugates, K.L. Johnson, G.C. Engelmayr Jr., Laser microfabricated poly (glycerol sebacate) scaffolds for heart valve tissue engineering, J. Biomed. Mater. Res. A 101 (2013) 104–114, https://doi.org/10.1002/jbm.a.34305.
[214] A. Patel, A.K. Gaharwar, G. Iviglia, H. Zhang, S. Mukundan, S.M. Mihaila, D. Demarchi, A. Khademhosseini, Highly elastomeric poly (glycerol sebacate)-co-poly (ethylene glycol) amphiphilic block copolymers, Biomaterials 34 (2013) 3970–3983, https://doi.org/10.1016/j.biomaterials.2013.01.045.
[215] C.L. Cummings, D. Gawlitta, R.M. Nerem, J.P. Stegemann, Properties of engineered vascular constructs made from collagen, fibrin, and collagen–fibrin

mixtures, Biomaterials 25 (2004) 3699–3706, https://doi.org/10.1016/j.biomaterials.2003.10.073.
[216] A.P. Breidenbach, N.A. Dyment, Y. Lu, M. Rao, J.T. Shearn, D.W. Rowe, K.E. Kadler, D.L. Butler, Fibrin gels exhibit improved biological, structural, and mechanical properties compared with collagen gels in cell-based tendon tissue-engineered constructs, Tissue Eng. A 21 (2014) 438–450, https://doi.org/10.1089/ten.TEA.2013.0768.
[217] E.D. Boland, G.E. Wnek, D.G. Simpson, K.J. Pawlowski, G.L. Bowlin, Tailoring tissue engineering scaffolds using electrostatic processing techniques: a study of poly (glycolic acid) electrospinning, J. Macromol. Sci., Part A 38 (2001) 1231–1243, https://doi.org/10.1081/MA-100108380.
[218] H.-Y. Mi, M.R. Salick, X. Jing, B.R. Jacques, W.C. Crone, X.-F. Peng, L.-S. Turng, Characterization of thermoplastic polyurethane/polylactic acid (TPU/PLA) tissue engineering scaffolds fabricated by microcellular injection molding, Mater. Sci. Eng. C 33 (2013) 4767–4776, https://doi.org/10.1016/j.msec.2013.07.037.
[219] J.M. Gere, S. Timoshenko, Mechanics of Materials Brooks, Cole, Pacific Grove, CA, 2001, pp. 815–839.
[220] D.C. Gloeckner, K.L. Billiar, M.S. Sacks, Effects of mechanical fatigue on the bending properties of the porcine bioprosthetic heart valve, Am. Soc. Artif. Intern. Organs J. 45 (1999) 59–63.
[221] A. Mirnajafi, J.M. Raymer, L.R. McClure, M.S. Sacks, The flexural rigidity of the aortic valve leaflet in the commissural region, J. Biomech. 39 (2006) 2966–2973, https://doi.org/10.1016/j.jbiomech.2005.10.026.
[222] K. Ragaert, F. De Somer, P. Somers, I. De Baere, L. Cardon, J. Degrieck, Flexural mechanical properties of porcine aortic heart valve leaflets, J. Mech. Behav. Biomed. Mater. 13 (2012) 78–84, https://doi.org/10.1016/j.jmbbm.2012.04.009.
[223] C. Martin, T. Pham, W. Sun, Significant differences in the material properties between aged human and porcine aortic tissues, Eur. J. Cardiothorac. Surg. 40 (2011) 28–34, https://doi.org/10.1016/j.ejcts.2010.08.056.
[224] Y. Chen, Y. Li, D. Xu, W. Zhai, Fabrication of stretchable, flexible conductive thermoplastic polyurethane/graphene composites via foaming, RSC Adv. 5 (2015) 82034–82041, https://doi.org/10.1039/C5RA12515D.
[225] A. Caballero, W. Mao, R. McKay, C. Primiano, S. Hashim, W. Sun, New insights into mitral heart valve prolapse after chordae rupture through fluid–structure interaction computational modeling, Sci. Rep. 8 (2018) 17306, https://doi.org/10.1038/s41598-018-35555-5.
[226] M.Y. Emmert, B.A. Schmitt, S. Loerakker, B. Sanders, H. Spriestersbach, E.S. Fioretta, L. Bruder, K. Brakmann, S.E. Motta, V. Lintas, Computational modeling guides tissue-engineered heart valve design for long-term in vivo performance in a translational sheep model, Sci. Transl. Med. 10 (2018) eaan4587, https://doi.org/10.1126/scitranslmed.aan4587.
[227] S. Naficy, G.M. Spinks, G.G. Wallace, Thin, tough, pH-sensitive hydrogel films with rapid load recovery, ACS Appl. Mater. Interfaces 6 (2014) 4109–4114, https://doi.org/10.1021/am405708v.
[228] H. Zhang, H. Xia, Y. Zhao, Poly(vinyl alcohol) hydrogel can autonomously self-heal, ACS Macro Lett. 1 (2012) 1233–1236, https://doi.org/10.1021/mz300451r.
[229] A. Phadke, C. Zhang, B. Arman, C.-C. Hsu, R.A. Mashelkar, A.K. Lele, M.J. Tauber, G. Arya, S. Varghese, Rapid self-healing hydrogels, Proc. Natl. Acad. Sci. 109 (2012) 4383–4388, https://doi.org/10.1073/pnas.1201122109.
[230] Q. Wang, J.L. Mynar, M. Yoshida, E. Lee, M. Lee, K. Okuro, K. Kinbara, T. Aida, High-water-content mouldable hydrogels by mixing clay and a dendritic molecular binder, Nature 463 (2010) 339, https://doi.org/10.1038/nature08693.
[231] C.-Y. Yang, B. Song, Y. Ao, A.P. Nowak, R.B. Abelowitz, R.A. Korsak, L.A. Havton, T.J. Deming, M.V. Sofroniew, Biocompatibility of amphiphilic diblock copolypeptide hydrogels in the central nervous system, Biomaterials 30 (2009) 2881–2898, https://doi.org/10.1016/j.biomaterials.2009.01.056.